MESOSCALE CIRCULATIONS IN THE URBAN-COASTAL ENVIRONMENT:

A MODELING ANALYSIS AND ASSESSMENT OF SENSITIVITY TO HIGH FIDELITY REPRESENTATION OF THE URBAN CANOPY

by

WILLIAM MICHAEL CARTER

(Under the Direction of J. Marshall Shepherd)

ABSTRACT

The overlap of urban and coastal atmospheric forcing mechanisms generates complex mesoscale circulations that are not easily interrogated using direct observational techniques. This study uses the WRF-ARW mesoscale model coupled to the NOAH land surface model to conduct a series of simulations of a study area centered on Houston, TX in order to characterize these circulations. The results of these simulations are used to construct a conceptual model of urban-coastal circulations describing the evolution of the sea breeze front and convective pump. Additionally, a series of urban canopy parameters derived using remote sensing techniques were used to create an enhanced representation of urban land cover within the model which was found to reduce bias in the model simulation when compared with actual ground observations taken within the urban area. The impacts of these urban-coastal circulations were also assessed with regard to transport of atmospheric pollutants and contaminants.

INDEX WORDS: Urban, Coastal, WRF, Urban Canopy Parameters, Sea Breeze, Convective Pump.

MESOSCALE CIRCULATIONS IN THE URBAN-COASTAL ENVIRONMENT: A MODELING ANALYSIS AND ASSESSMENT OF SENSITIVITY TO HIGH FIDELITY REPRESENTATION OF THE URBAN CANOPY

by

WILLIAM MICHAEL CARTER

B.S., Mississippi State University, 2007

A Thesis Submitted to the Graduate Faculty of The University of Georgia in Partial Fulfillment of the Requirements for the Degree

MASTER OF SCIENCE

ATHENS, GEORGIA

2009

MESOSCALE CIRCULATIONS IN THE URBAN-COASTAL ENVIRONMENT: A MODELING ANALYSIS AND ASSESSMENT OF SENSITIVITY TO HIGH FIDELITY REPRESENTATION OF THE URBAN CANOPY

by

WILLIAM MICHAEL CARTER

Major Professor: J. Marshall Shepherd

Committee: Thomas L. Mote
Andrew J. Grundstein

Electronic Version Approved:

Maureen Grasso
Dean of the Graduate School
The University of Georgia
May 2009

ACKNOWLEDGEMENTS

This work would not have been possible without the support of the excellent faculty and staff of the University of Georgia Department of Geography. I would like to especially thank the members of my thesis committee and my superlative advisor, J. Marshall Shepherd. I could not have asked for a better mentor during my time here. I would also like to thank Steve Burian of the University of Utah and his team whose urban canopy data set was an integral part of this study. I gratefully acknowledge the assistance of the Southern High Resolution Modeling Consortium (SHRMC) in providing computing resources, partially supported by contract AG-4568-C-08-0063 to Thomas L. Mote, University of Georgia. Finally, I would like to thank the Defense Threat Reduction Agency for their generous support and funding of this work.

TABLE OF CONTENTS

Page

LIST OF TABLES

Page

LIST OF FIGURES

Page

CHAPTER 1

INTRODUCTION

Urbanization is increasing around the globe. According to the United Nations Population Fund, in 2008 humanity will have reached a critical point in its history in that for the first time more than half of the world's population, over 3.3 billion people, will be living in urban areas. This trend is expected to continue to the extent that by 2030 the number of people living in urban areas could reach 5 billion (UNPF 2007). Humankind's ever expanding urban footprint has broad ranging implications on many fronts including surface energetics, water and carbon cycle processes, and ecosystem development. Urbanization has also been shown to have a profound effect on weather and climate on local and regional scales. It has been known since the early days of modern meteorology that urbanization has an effect on local temperature distribution. Climatologist Luke Howard first measured this urban to rural temperature gradient in his 1833 book, *Climate of London.* The urban effect on temperature was first termed the "urban heat island" by Gordon Manley in 1958. Urban effects are not limited to temperature however; past studies have also found links to precipitation anomalies and changes in atmospheric circulation from the mesoscale to the microscale (Fig. 1.1) (Shepherd, 2005).

Concurrent with this increase in urbanization has been an increase in coastal population density. The US Department of Commerce's National Oceanic and Atmospheric Administration (NOAA) cites that 53% of the population of the United States lives in coastal counties that make up only 17% of its land area (Crossett et al, 2004). Coastlines, like cities, tend to be dominant

forcing mechanisms on local weather and climate. Thus the places where these littoral and urban atmospheric processes overlap are becoming an increasingly important area of research for mesoscale weather phenomena, atmospheric dispersion and transport.

The issues involved in forecasting urban-coastal interactions are complex, and perhaps nowhere are their impacts more evident than in Houston, TX (Fig. 1.2). Houston is one of the most rapidly growing coastal cities in the US (Fig. 1.3), and is also a major center of the international petrochemical industry. Houston's position in relation to the Gulf of Mexico and the unique morphology of Galveston Bay cause complex coastal circulation patterns to evolve near the city. Coupled with the circulations generated by the urban heat island (UHI), this complex flow regime often results in the advection of atmospheric pollutants, which are largely byproducts of the petrochemical refinement process, into the more densely populated metropolitan area (Fig. 1.4) (Banta, et al. 2005). However, these patterns of advection are not well predicted by current forecasting methods due to poor representation of the urban canopy and the coarse resolution of numerical weather prediction models. Further, urban-sea breeze mesoscirculations alter dispersion and transport patterns of chemical, biological, and radiological agents and are of interest because of their implications for homeland and national security concerns. It is the goal of this study to create a new framework for characterizing urban coastal circulations.

1.1 Motivation

1.1.1 *Increased Spatial Resolution*

Numerical simulations have been shown to be a useful approach in better understanding urban-coastal circulations. Nielsen-Gammon (2000), using the Penn State/NCAR Mesoscale Model Version 5 (MM5) (Grell et al. 1994), was able to simulate the Houston sea breeze front using 4km grid resolution. He states that the development of small scale sea breeze structures is dependent on the model grid resoulution, which is directly related to the degree of detail that can be represented in the coastal morphology. Furthermore, he states that, at minimum, a resolution of 3km is required to develop a strong sea breeze front. In order to better understand these complex sea breeze structures, it is necessary to perform simulations using much higher spatial resolution, on the order of 1km. This study has been able to achieve these resolutions using the WRF-ARW numerical weather prediction model, described in detail later, to conduct a series of simulations initiated from the 32km North American Regional Reanalysis (NARR) dataset. A series of three nested domains within the large-scale model allows for a final resolution of approximately 1.2 km over the study area. As will be shown, this resolution is sufficient to capture the sea breeze front and associated convergence patterns crucial to understanding urban-coastal circulations.

1.1.2 *Increased Urban Canopy Parameter Resolution*

Along with spatial resolution, accurate representation of the urban environment within atmospheric models is dependent on a series of urban canopy parameters (UCPs). These parameters account for the aspects of the urbanized environment that have an effect on

atmospheric circulation, such as the increased mechanical turbulence from tall buildings, the albedo of paved surfaces, and the urban canyon effect. Therefore, in order to produce the most realistic simulation possible of urban induced circulations, it is necessary to include as accurate a depiction as possible of the urban landscape. Holt and Pullen (2006) specifically cite "improving our understanding of the sensitivity of urban parameterizations to the specification of the urban morphology within the model" as a future research need. By using the WRF Urban Canopy Model (Kusaka and Kimora 2004) along with the NOAH Land Surface Model (Ek et al. 2003), this study has been able to incorporate a high resolution UCP data set derived using remote sensing techniques into the WRF-ARW simulations, resulting in a much more accurate representation of an urban area than has been achieved previously. This is one of the first studies to incorporate a high resolution urban canopy parameter data set of this type for purposes of atmospheric modeling.

1.1.3 *Understanding Urban-Coastal Circulations*

By incorporating both a high degree of spatial resolution and a better representation of the urban environment itself through the use of remotely-sensed UCPs, this study has been able to produce a very accurate depiction of the urban-costal circulations present in the Houston metropolitan area. This high fidelity representation has many benefits for the increased understanding of urban and coastal weather processes and has implications in the fields of weather forecasting, air quality and pollutant advection, urban induced climate phenomena, and national security concerns such as the transport of biological, chemical, and radiological contaminants in urban environments.

1.2 Research Objectives

The primary objectives of this research are as follows:

- To determine whether the city of Houston generates an enhanced convergence zone and associated convective pump mechanism.
- To determine the role of urban induced forcings and coastal morphology in the development and evolution of the sea breeze and associated mesoscale boundary.
- To determine the impact of detailed representation of the urban land surface on simulations of the regional dynamic and thermodynamic circulations in the Houston area.

This thesis addresses the aforementioned objectives by comparing a series of model simulations of the atmosphere within a study area centered on the city of Houston, TX during a specified case period. The results of these simulations are analyzed for various dynamic and thermodynamic mechanisms which identify and characterize the complex mesocirculations which are taking place.

The first objective of this research is to demonstrate the existence of an enhanced convergence zone leading to the formation of a convective pump and associated positive vertical motion field over the Houston area, while simultaneously determining the relative role of urbanization (e.g., heat island circulation, roughness) in generating this enhanced convergence. It is hypothesised that the surface and upper air conditions in the Houston metropolitan area will show evidence of increased convergence and low-level instability in and around the urban environment leading to the formation of a convective pump.

The second objective of this research is to characterize what role, if any, urban induced atmospheric perturbations have on the evolution of the sea breeze front, and to separate out the effects these mechanisms from those generated by the complex coastal morphology. It is hypothesised that two key attributes of the urban-sea-bay breeze mesocirculation, the intensity and timing of the sea breeze front, are partially a function of urban land cover.

The third objective of this research is to determine the importance of a detailed representation of the urban land surface to the regional dynamic and thermodynamic circulations in the Houston, TX area, and by extension the effects of this high fidelity urban representation on simulations of parcel trajectories which are important for the transportation of atmospheric pollutants or contminants. It is hypothesised that the inclusion of urban canopy parameters derived using remote sensing techniques into coupled WRF-NOAH simulations will have significant effects on the representation of urban/coastal induced circulations, convergence, and vertical motion. This section represents a particularly novel component of the thesis and is one of the first demonstrations of the value of remotely-sensed UCPs in WRF simulations.

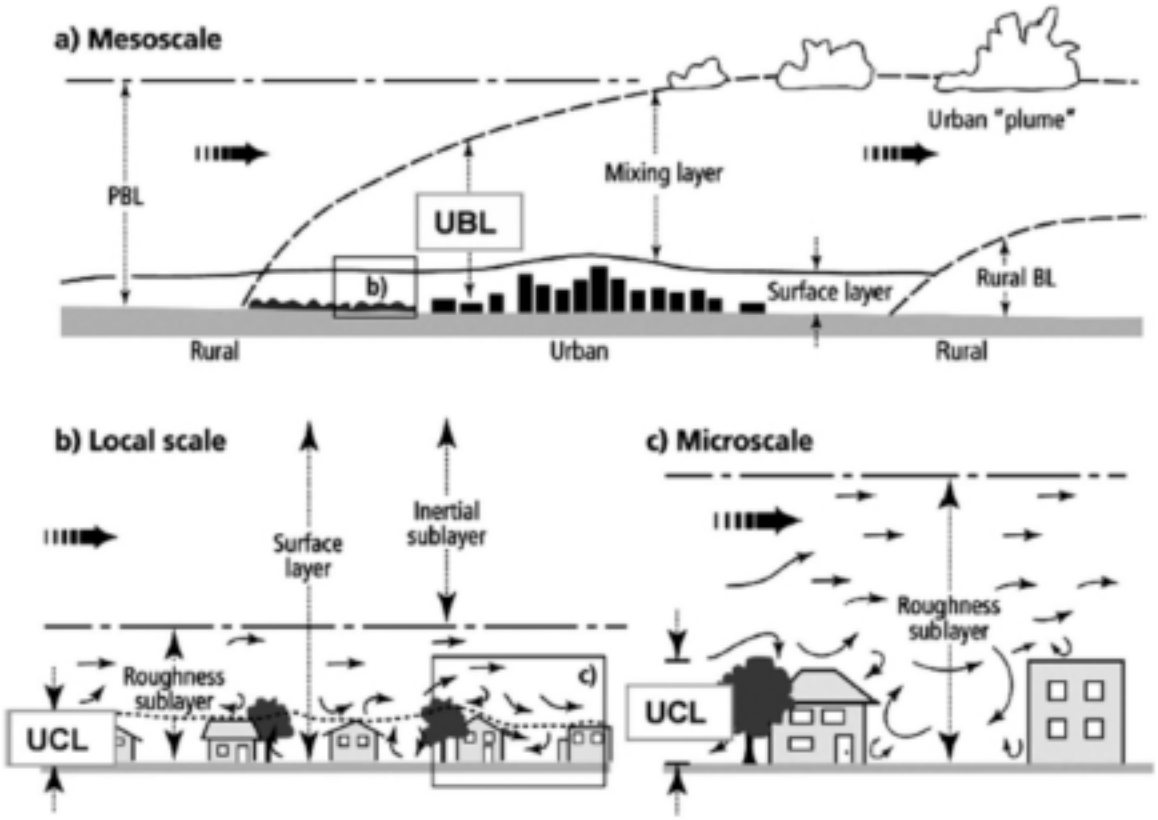

Fig. 1.1. Effects of the urban canopy on mesoscale, local scale, and microscale atmospheric circulations (from Shepherd 2005 originally following Oke 1987).

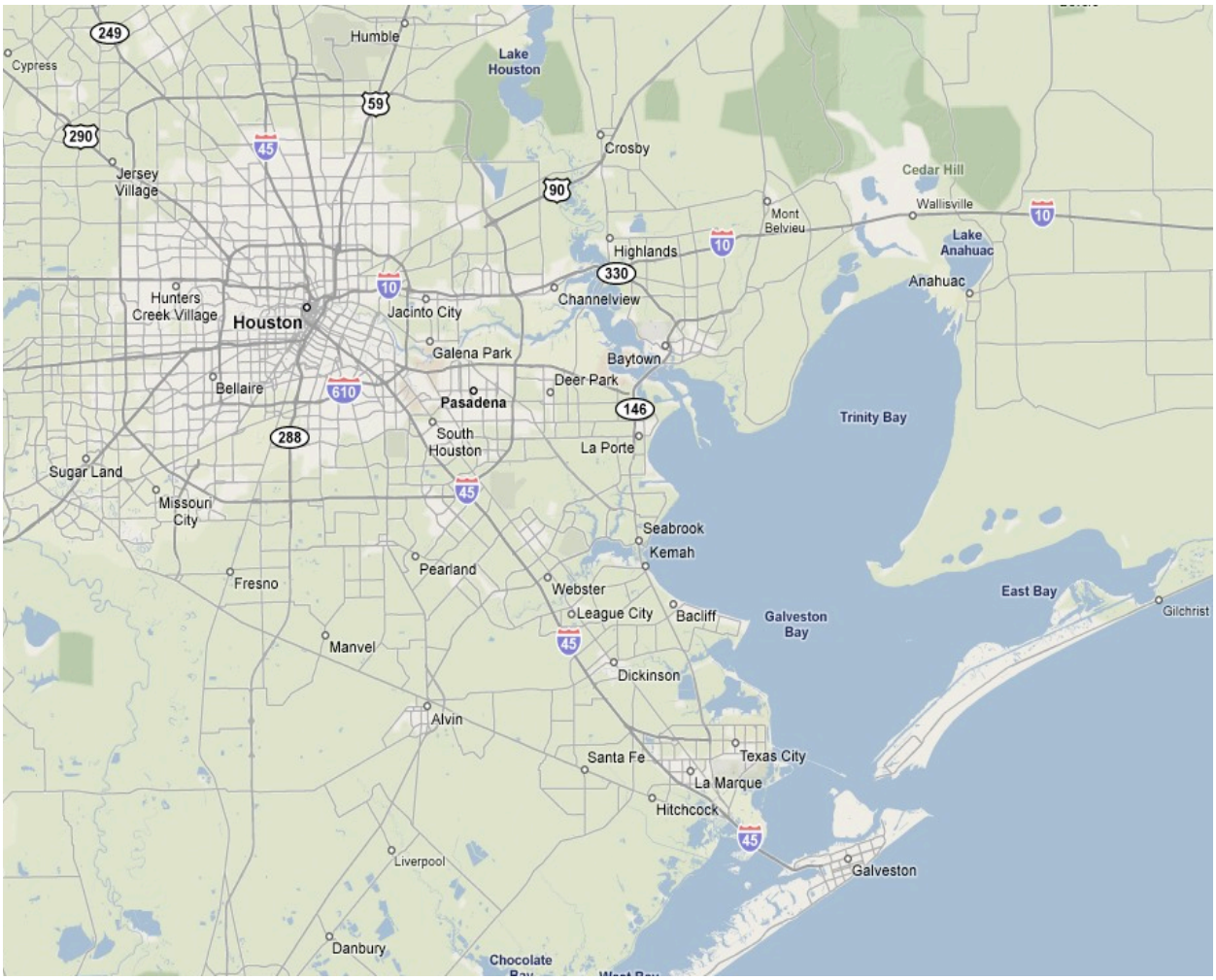

Fig. 1.2. The Houston, TX, metropolitan area and its relationship to Galveston Bay (from Google Earth).

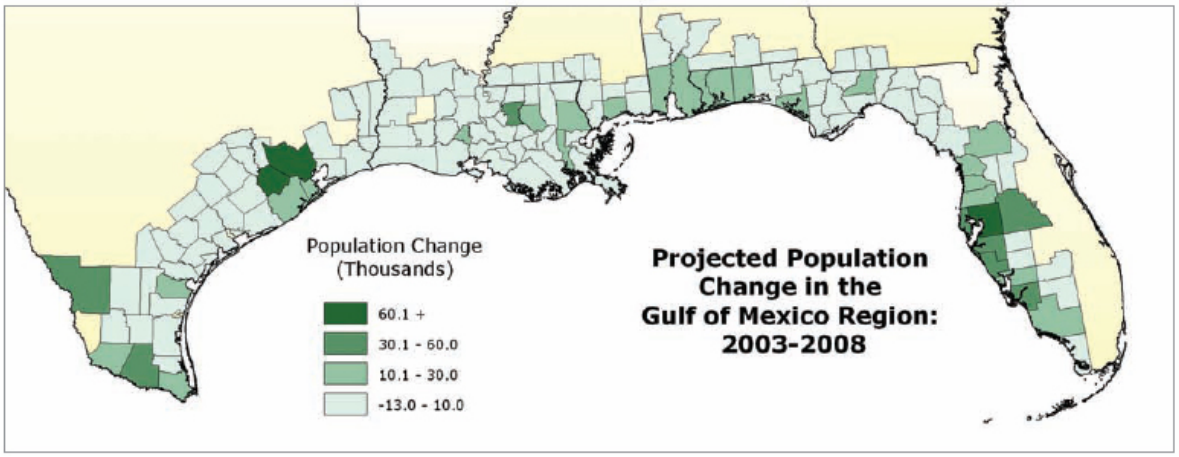

Fig. 1.3. Projected population change in the Gulf of Mexico Region: 2003-2008 (from Crossett et al. 2004).

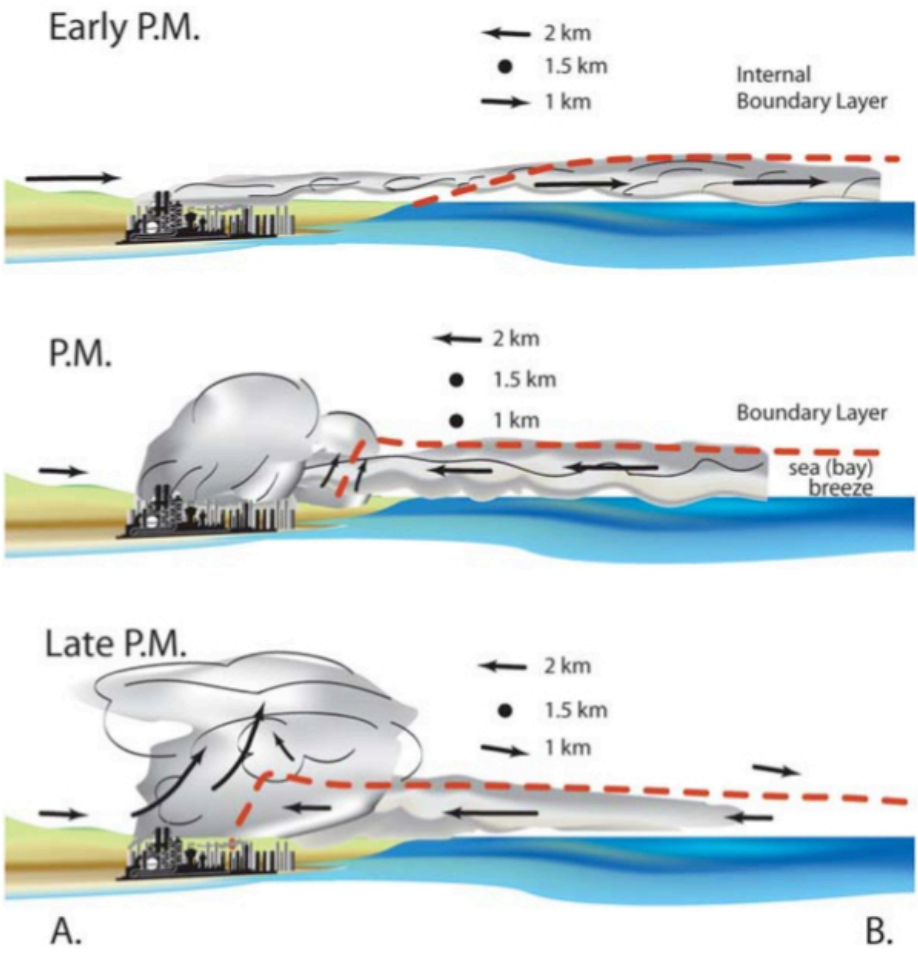

Fig. 1.4. Conceptual illustration of the complex flow patterns which set up over Houston as a result of the sea breeze circulation (from Banta et al. 2005).

CHAPTER 2

LITERATURE REVIEW

2.1 The Sea Breeze

The American Meteorological Society's Glossary of Meteorology (Glickman, 2000) defines the sea breeze as "a coastal local wind that blows from sea to land, caused by the temperature difference when the sea surface is colder than the adjacent land." Theoretical understanding of the sea breeze goes back as far as Haurwitz (1947). Holton (2004) further defines the sea breeze as an archetypal example of a pressure-density solenoid circulation. Fig. 2.1 illustrates how the sea breeze is initiated and maintained. Under conditions in which the sea surface temperature is cooler than the land surface temperature, which often occurs on summer days owing to the fact that the land surface warms more rapidly than the water due, among other factors, to its greater specific heat, the mean temperature through a layer from h_0 to h over water with mean temperature T_1 will be less than the mean temperature through the same layer over land, T_2. Assuming a constant surface pressure p_0, the height of a second pressure surface p_1 will therefore be greater over land than over water given that variation in geopotential height with respect to pressure is dependent only on temperature, as described by the hypsometric equation (Holton 2004). Thus the isobaric surfaces will begin to tilt downward toward the ocean, and at a given altitude above the surface z, a pressure gradient force will exist causing wind to blow from

the landward direction out to sea. This land breeze above the surface is what instigates the coastal circulation; with divergence above the land leading to rising motions and relatively lower surface pressure inland, and convergence above the water leading to subsidence and relatively higher surface pressure out to sea. The circulation loop is then completed by the initiation of flow from sea to land near the surface, which is what we recognize as the sea breeze. This circulation will continue until the land-sea temperature contrast is weakened or even reversed after sunset.

Limiting factors on the sea breeze circulation include surface friction and weakening of the coastal temperature gradient due to thermal advection by the sea breeze itself. According to Banta (2005), the strength of the sea breeze is directly related to latitude in that the sea breeze is strongest when the diurnal forcing mechanisms are synchronized with the Coriolis force. Banta found 30 degrees latitude to be the ideal location for strong sea breeze development, thus Houston, located just equatorward of 30 degrees, has a particularly strong sea breeze influence. However, the sea breeze is a mesoscale phenomenon, and as such relies on relatively weak forcing mechanisms in comparison to the large-scale synoptic flow. Therefore, the sea breeze is most prevalent on synoptically quiescent days, and the sea breeze signal can be mitigated or washed out completely by the dominant synoptic flow.

2.2 The Sea Breeze Front and Houston

A unique feature of the sea breeze is the sea breeze front, which, according to the AMS Glossary, is the "horizontal discontinuity in temperature and humidity that marks the leading edge of the intrusion of cooler, more moist marine air associated with the sea breeze." Banta et al. (2005) described the evolution of the Houston sea breeze front. Under the proper conditions,

the mesoscale boundary begins to develop in the morning as the land-sea temperature contrast sharpens and the sea breeze circulation sets up. Depending on a number of factors, This boundary can progress inland less than 100 km or more than 300 km at the peak of its diurnal cycle (Simpson, 1994). The sea breeze front follows the contours of the sea coast and can generate patterns of convergence and divergence that greatly affect the mesoscale environment. In general, sea breeze fronts that follow convex coastlines lead to enhanced convergence, while sea breeze fronts that follow concave coastlines lead to enhanced divergence. As the sea breeze progresses inland, convergence zones develop landward of the two headlands on either side of Galveston Bay (Smith Point to the north and Texas City to the south) as the sea breeze front turns in on itself, while at the same time a generally divergent regime sets up over the city itself, due to the concave shape of the interior part of the bay. McPherson (1970) found a region of preferred thunderstorm initiation and enhancement in the aforementioned convex regions around Galveston Bay. Complicating this simple model of convergence and divergence zones however, is the city of Houston itself, which has its own effects on the local environment largely attributed to the UHI. McPherson's work did not explicitly resolve urban land cover.

2.3 Urban Heat Island Dynamics

As stated to earlier, the UHI has a long history in the literature. Urban climatologies have shown that the urban rural temperature contrast can be as much as 10°C (Bornstein and Oke, 1980, Oke 1981, Bornstein 1987, Ohashi and Kida, 2002). Souch and Grimmond (2006) summarize much of the previous research on the characteristics of the UHI, stating that it reaches its diurnal peak during the nighttime hours, that it can be limited by increased wind

speed and cloud cover, that its intensity varies by season with the minimum signal occurring in summer, and that it is strongly related to surface/building geometry, land use, vegetation and patterns of anthropogenic heat release. The thermal and dynamic effects of the UHI have been linked to many weather phenomena, but of particular interest to this study are the enhanced convergence zones that exist around the periphery of UHIs. Hjelmfelt (1982) simulated the UHI of St. Louis and found positive vertical velocities downwind of the city. He argued that the enhanced surface roughness convergence effect and the downwind shifting or enhancement of the UHI circulation by the synoptic flow were the cause. More recent investigation into this UHI induced convergence continued to find unique patterns of thunderstorm initiation and development near cities, such as Bornstein and Lin's (2000) finding that thunderstorms tended to diverge around Atlanta, GA, or initiate due to enhanced convergence zones. Rozoff et al. (2003) also found that a strong convergence zone existed leeward of St. Louis, MO, as well as a weaker convergence zone on the windward side of the city. This urban convergence zone and associated thunderstorm development has been posited as a potential cause of urban-induced precipitation anomalies. Shem and Shepherd (2009) found evidence of enhanced convergence on the inner periphery of Atlanta's urban land cover.

2.4 The Convective Pump

Recent studies, including an unpublished study by Nielsen-Gammon (2000), suggest that a third dynamic mechanism in urban-coastal systems is caused by thermally driven vertical motions over the city itself. Herein called the convective pump, this vertical motion field is of particular interest to this study, as it combines aspects of both urban and coastal circulation

forcing mechanisms. As the air over the city rises due to its relatively higher temperatures as compared to the surrounding area, a return flow sets up near the surface to replace the evacuated mass (Fig 2.2). This circulation and associated vertical motion field were found by Nielsen-Gammon to combine with the sea-breeze flow near Houston, forming a continuous band of southeasterly winds between the city and Galveston Bay. Furthermore, the rising motion and associated enhanced convergence was found to be a cause for thunderstorm initiation, similar to Shepherd et al. (2001), as well as a pollutant transport mechanism.

2.5 Previous Modeling Work on the Urban-Coastal System

Efforts to model complex urban-coastal systems have been successfully completed (Yoshikado 1992, Yoshikado 1994, Kitada et al. 1998, Kusaka et al. 2000, Ohashi and Kida 2002, Lo et al. 2007). The primary findings of these studies are that 1) urban-coastal circulations can be successfully simulated using a coupled atmosphere-urban canopy model (Kusaka et al. 2000); 2) large cities like Hong Kong contribute to an enhanced coastal temperature gradient; 3) large urbanized areas (> 10km) create thermal circulations in the mesoscale leading to enhanced vertical motions where the UHI and sea-breeze front converge and; 4) if an inland urban area exists, the combined urban-coastal circulation is stronger and lasts longer than a typical sea breeze (Ohashi and Kida, 2002). These studies primarily focused on cities outside of the US, and Nielsen-Gammon's Houston work has not been published in the refereed literature. Also, while these studies have focused on sea-breeze UHI interactions, none have incorporated an urban canopy parameter data set derived from direct measurements of the urban environment in question.

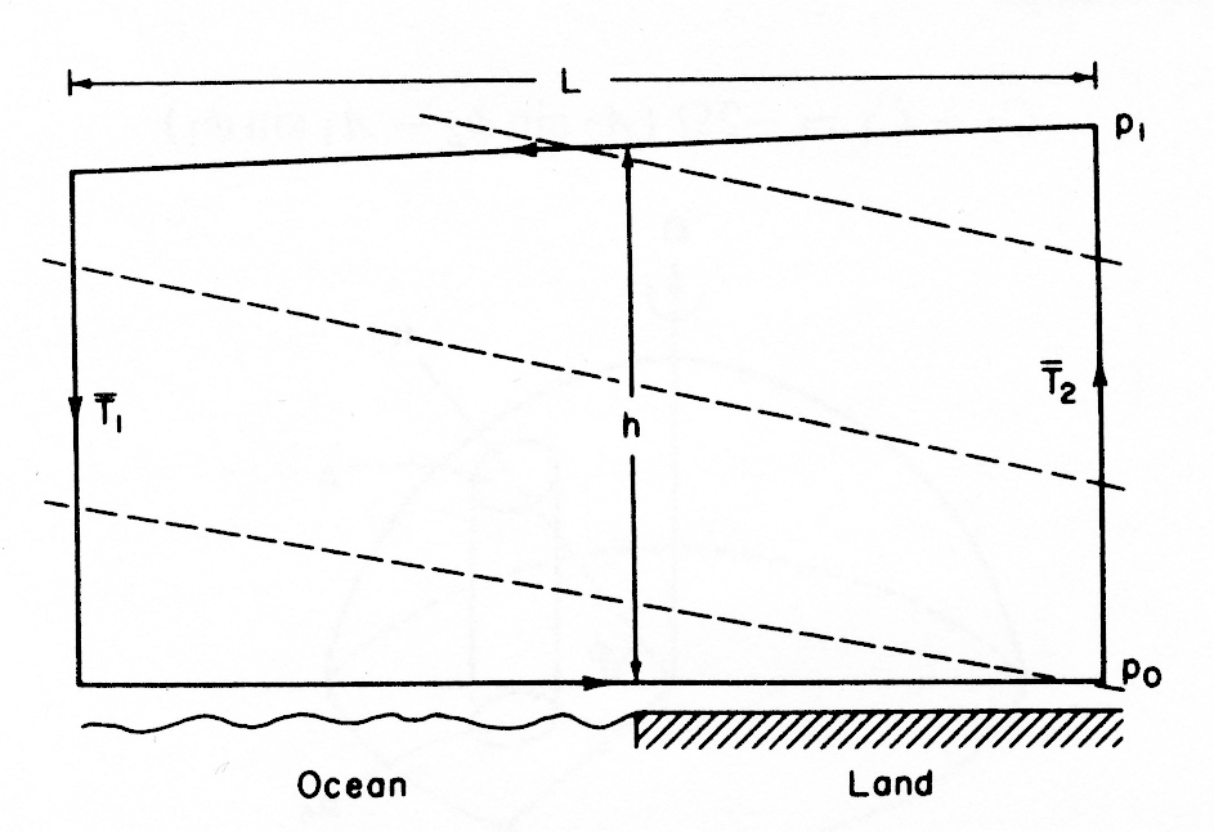

Fig. 2.1. Illustration of the basic model of sea breeze formation (from Holton 2004).

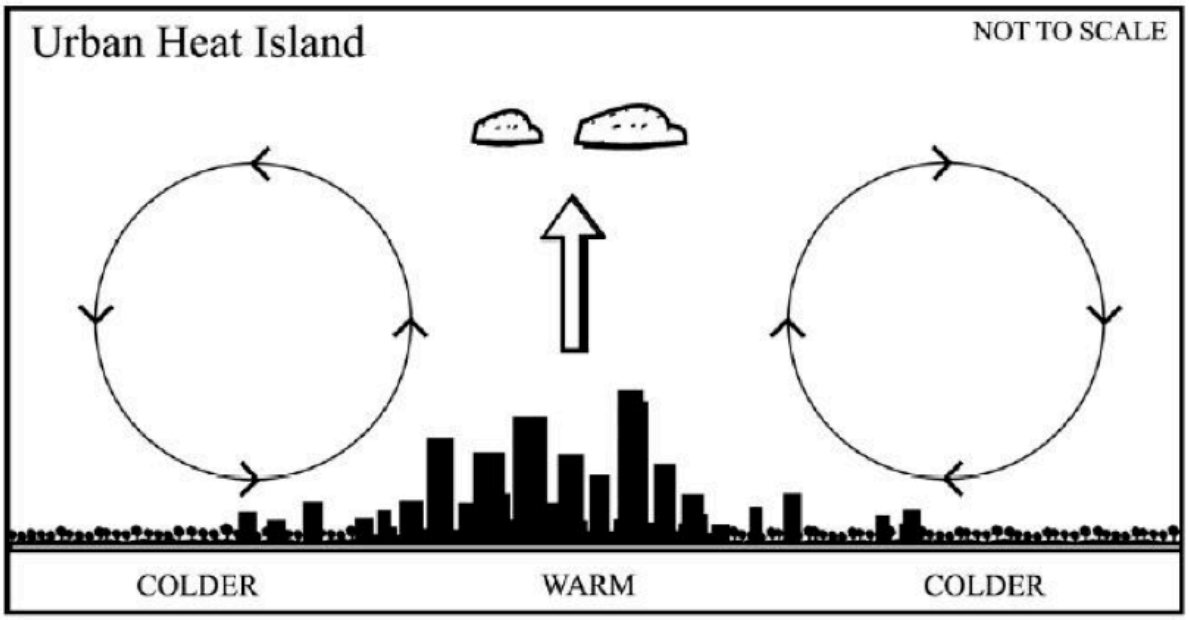

Fig. 2.2. Illustration of the positive vertical motion field and low level convergence initiated by the urban heat island (from Simpson 2006).

CHAPTER 3

RESEARCH DESIGN AND METHODS

3.1 Study Area and Case Period

The study area for this project is a region approximately 175 km by 175 km centered over the city of Houston, TX, which also includes Galveston Bay and much of the nearby coastline (Fig. 3.1). This comprises the fourth domain of the various WRF simulations used herein (Fig. 3.2). This domain is represented within the model as a 160 by 160 point grid with 27 vertical levels.

The study employs a case study approach. Case studies are commonly used to investigate physical mechanisms within a convective-mesoscale framework. While results must be carefuly interpreted and not generalized, the literature is overwhelmingly clear concerning the contributions of properly designed case studies using models. This study focuses primarily on one specific case period: 17-18 August 2006. This case was chosen based on two criteria, the first of which is the suitability of the synoptic and mesoscale weather conditions. Analysis of satellite data, surface weather observations, Doppler radar, and operational forecast model products shows that for these case days, there existed a well developed sea breeze circulation, as well as an absence of large scale synoptic forcing mechanisms. Thus, any circulations that we are able to resolve should be due to the mesoscale environment primarily. The second criteria was that the case study days fall within the study period of the Second Texas Air Quality Survey

(TexAQS II) campaign. TexAQS II (Cowling and Parrish 2006) was an intensive effort to measure air quality and pollutant transport in southeast Texas using a dense network of surface and upper air data collection systems (Fig 3.3). While the primary focus of the TexAQS II campaign was air quality, and thus a large portion of the data collected was related to atmospheric pollutants such as ozone, all of the surface monitoring stations also collected basic meteorological data including temperature, dew point temperature, wind speed and wind direction, which are used for model verification in this study. These data have been made available to us in digital format and can be accessed at http://atmo.tamu.edu/texaqs2/ (Nielsen-Gammon, 2009 personal communication).

3.2 Data

3.2.1 *WRF-NOAH*

This study utilizes a series of coupled WRF-NOAH simulations of the atmosphere. The WRF model was developed as a collaborative effort by the National Center for Atmospheric Research (NCAR), the National Centers for Environmental Prediction (NCEP), the Forecast Systems Laboratory (FSL), the Air Force Weather Agency (AFWA), Oklahoma University (OU) and the university community. The version of the model used is the Advanced Research WRF (WRF-ARW) version 2.2. The ARW dynamic core is designed to integrate the compressible, nonhydrostatic Euler equations using a terrain following mass vertical coordinate (Skamarock et al. 2005) and is structured to perform case studies based on real input data. The input data used in this case study is from the North American Regional Reanalysis (NARR) data set maintained by the National Centers for Environmental Prediction

(http://www.emc.ncep.noaa.gov/mmb/rreanl/). For each case, the model is run for the duration of the case study period, totaling 36 hours, ingesting updated input data every six hours, which simulates the assimilation of data from real world surface and upper air meteorological data sources. The NARR input data has a spatial resolution of 32 km, which is then enhanced by using a series of nested domains within the model. Each domain increases the resolution by a factor of three, such that the fourth domain, centered over Houston, has a resolution of 1.18 km.

In order to more accurately represent the effects of the urban environment and land surface interactions within the urban environment, the NOAH Land Surface Model (LSM) and WRF Urban Canopy Model (UCM) have been coupled to the WRF-ARW for these simulations. The NOAH LSM was developed by NCEP, Oregon State University, AFWA, and the National Weather Service Hydrologic Research Lab and is used to provide latent heat fluxes and surface skin temperature (Kusaka and Kimura 2004). The WRF UCM is used to represent the physical processes involved in the exchange of heat, momentum, and water vapor in urban environment by providing a representation within the model of shadowing from buildings, reflection of short and longwave radiation, wind profiles in the canopy layer and multi-layer heat transfer equations for roof, wall and road surfaces (Tewari, et al. 2007) (Figs. 3.4, 3.5).

Table 3.1 shows the physics and dynamics options used for the primary study area (4th domain):

Table 3.1. Physics and dynamics options used for the simulations described herein.

Option	**Selection**
microphysics	Ferrier
longwave radiation	RRTM
shortwave radiation	Dudhia scheme
surface layer	Monin-Obukhov scheme
surface physics	NOAH LSM
boundary layer physics	YSU scheme
cumulus parameterization	none
turbulence and mixing option	simple diffusion
eddy coefficient option	2D deformation

These are held constant throughout all the simulations used in this study, so that any differences between simulations should be due only to changes in the representation of urban land cover.

3.2.2 *Urban Canopy Parameters*

The urban canopy parameters used in this study originate from a unique data set provided by Steve Burian from the University of Utah. This data set is derived using Light Detection and Ranging (LIDAR) measurements of the urban environment (Burian, 2008 personal communication and DVD of National Building Statistics Database provided by S. Burian, University of Utah), and describes the physical characteristics of the urban landscape in great detail and at high resolution (Fig. 3.6). This study represents one of the first times a data set of

this type has been incorporated into a numerical weather prediction model to study urban-coastal circulations.

The specific urban canopy parameters which will be used are as follows (following recommendations of Holt and Pullen, 2006), building height (m), momentum roughness length above canyon (m), sky view factor (implicit). These parameters are argued by Holt and Pullen to be critical to sea breeze morphology. Further, they represent UCPs available in the Burian data set. A grid representing the model simulations' finest resolution was overlaid over the Burian data set and a mean value for each UCP was calculated for each cell. Then, a natural breaks classification was used to separate these cells into three new land classes, analogous to "low intensity residential," "medium intensity residential," and "industrial or commercial" in the standard USGS classification scheme, which are the land use classes expected by the urban canopy model (Fig 3.7). The classification was based solely on building height. A mean value of each of the UCPs was then calculated for each of these new UCP based land classes, and that value was used to replace the standard value within the urban canopy model's parameter table. For those UCPs which are not included in the Burian data set, the value from the analogous USGS land class was used, following Tewari et al. (2007). This new UCP based urban land cover data was overlaid on the standard USGS 30 arcsecond land cover to generate a new hybrid land cover data set which was used in the enhanced UCP simulations.

3.2.3 *Verification Data*

In order to validate the model simulations, meteorological data were used that were collected as part of the TexAQS campaign, as well as surface data from both the Automatic Surface Observation System (ASOS) network and the Texas Mesonet. Additional surface and satellite based observations were used in order to indentify a suitable case day. Comparisons of model results with observations are shown in Fig. 3.8 and 3.9 confirm that the simulations are realistically reproducing the mesoscale circulations on the selected day. Further, a statistical impact score (described in detail in section 3.3.3) was created to provide a quantitative method of model validation.

3.3 Research Methodology

3.3.1 *Convective Pump Identification*

In order to identify the presence of an urban induced convective pump, two model simulations were conducted, subsequently referred to as SimpleUrban and NoUrban. The original land cover dataset distributed with WRF-NOAH underestimates the extent of current urban land cover. Therefore, in the SimpleUrban scenario, the model is run using a hybrid land cover data set based on the USGS 30 arcsecond land cover overlaid with the expanded urban land cover for Houston derived from the Burian data set. These data are used to mantain a consistent urban land cover extent between this and subsequent runs, so that any differences between simluations will be due only to changes in urban land cover characteristics and not changes in spatial coverage. However, in the SimpleUrban run, no enhanced urban canopy parameters are used. In the NoUrban scenario, the entire Houston metropolitan area was

replaced in the simulation with dryland/cropland, which is the dominant land cover class of the surrounding area. By comparing these two runs, one with and one without the city in place, it is possible to show the direct effects on atmospheric circulation caused by the urban area. The following parameters were then analyzed in order to detect the presence of an urban indcued convective pump: skin temperature, convergence, vertical velocity, and Bulk Richardson Number (BRN) shear. The BRN shear value is the denominator of the Bulk Richardson Number equation and is representative of the difference between a density weighted mean wind speed taken over the lowest 6km of the profile and an average near-surface wind speed taken over the lowest 500m of the profile, as:

$$\text{BRN Shear} = 0.5 * (u_{6km} - u_{500m})^2 \quad (3.1)$$

where u_{6km} is the 0-6 km density weighted mean wind and u_{500m} is the 0-500 m density weighted mean wind. Weisman and Klemp (1982) equate the BRN shear with the "inflow kinetic energy" of a thunderstorm updraft. Here it is used in a similar fashion to identify the convective upwelling of parcels associated the the convective pump.

3.3.2 *Sea Breeze Evolution*

In order to characterize changes in the sea breeze and sea breeze front due to interaction with the urban area, the same SimpleUrban and NoUrban simulations are used. The sea breeze front is identified based on the vertical velocity anomaly that occurs at this mesoscale boundary interface. Inland penetration, morphology, and dwell time, or amount of time the sea breeze

boundary is in contact with the urban area, of the sea breeze front are evaluated. Differences are identified between the SimpleUrban and NoUrban scenarios to determine the relative roles of urbanization and coastal morphology in sea breeze evolution.

3.3.3 *Sensitivity to Urban Canopy Parameters*

In order to characterize the sensitivity of these simulations to enhanced representation of the urban canopy, as well as identify possible implications regarding convective pump evolution and pollutant and contaminant transport, a third simulation was conducted, hereafter referred to as UCPUrban. This simulation is similar to the SimpleUrban scenario, however the enhanced land classes and associated urban canopy parameter values derived from the Burian dataset were incorporated into the land use data set. A statistical impact score was derived to identify the effect of enhanced urban canopy parameters on the diurnal temperature cycle, which is as:

$$\text{Impact Score} = \sigma_{\text{SimpleUrban.Bias}} - \sigma_{\text{UCPUrban.Bias}} \tag{3.2}$$

where

$$\sigma = \sqrt{\frac{\sum_{k=1}^{n} (x_k - \mu)^2}{n}} \tag{3.3}$$

in which x is the observed bias at each time and μ is the mean bias over all times.

The 2m air temperature from the SimpleUrban and UCPUrban were subtracted from the same values from selected TexAQS observation sites in order to create a measure of bias. That bias

was then standardized by calculating the root mean square error and compared to identify the impact of enhanced urban canopy parameters at a series of TexAQS sites. Differences in the evolution of the convective pump, skin temperature, and parcel trajectories between the SimpleUrban and UCPUrban scenarios were investigated. The results of these various analyses are presented in Chapter 4.

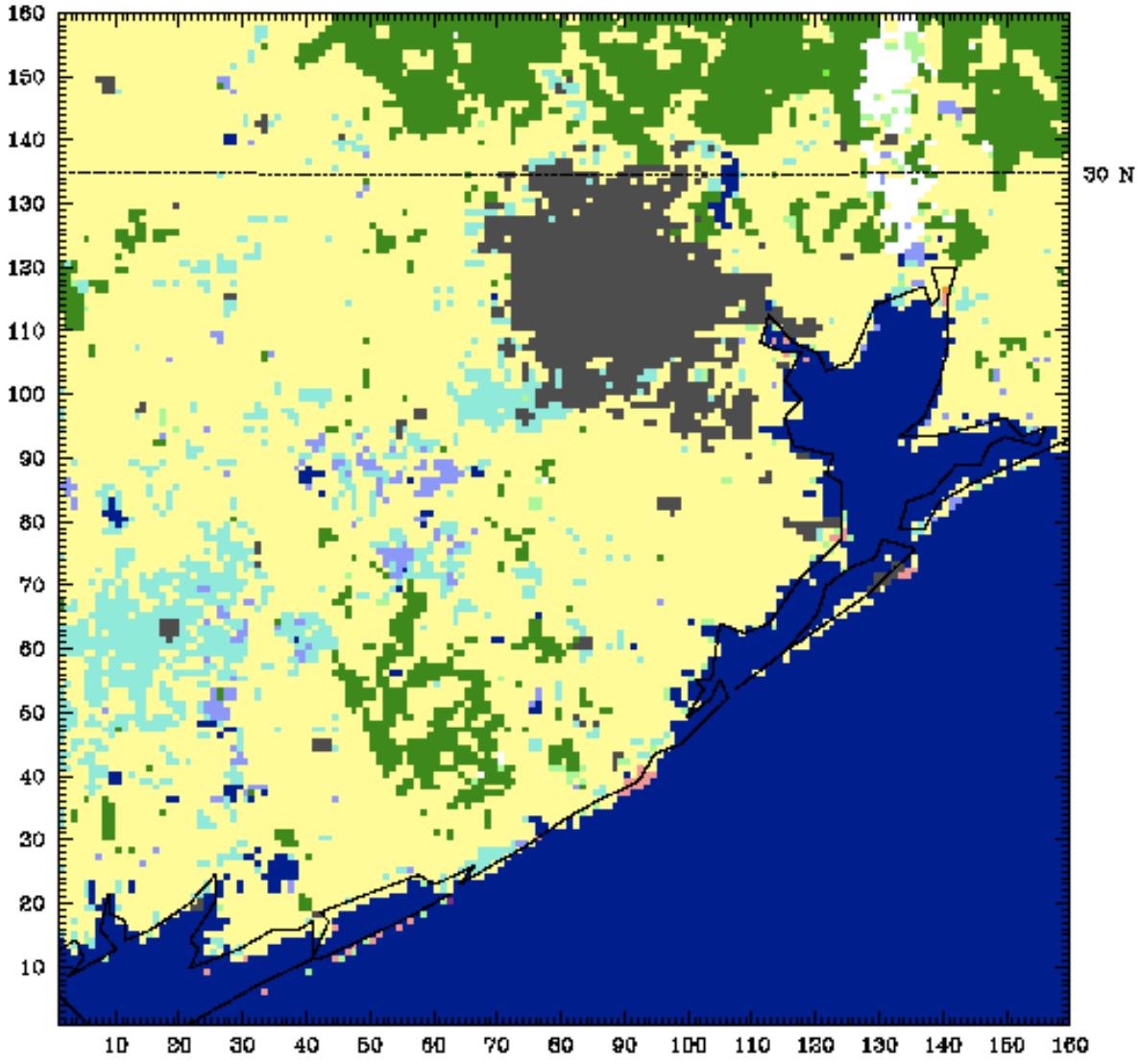

Fig. 3.1. Representation of the study area comprising the fourth domain of the WRF simulations used herein. Each pixel represents one model grid cell. The land cover types represented are urban (gray), evergreen needleleaf (dark green), dryland-cropland pasture (yellow), deciduous broadleaf (white), crop-grass mosaic (light green), mixed dry-irrigated pasture (lavender) and water (blue).

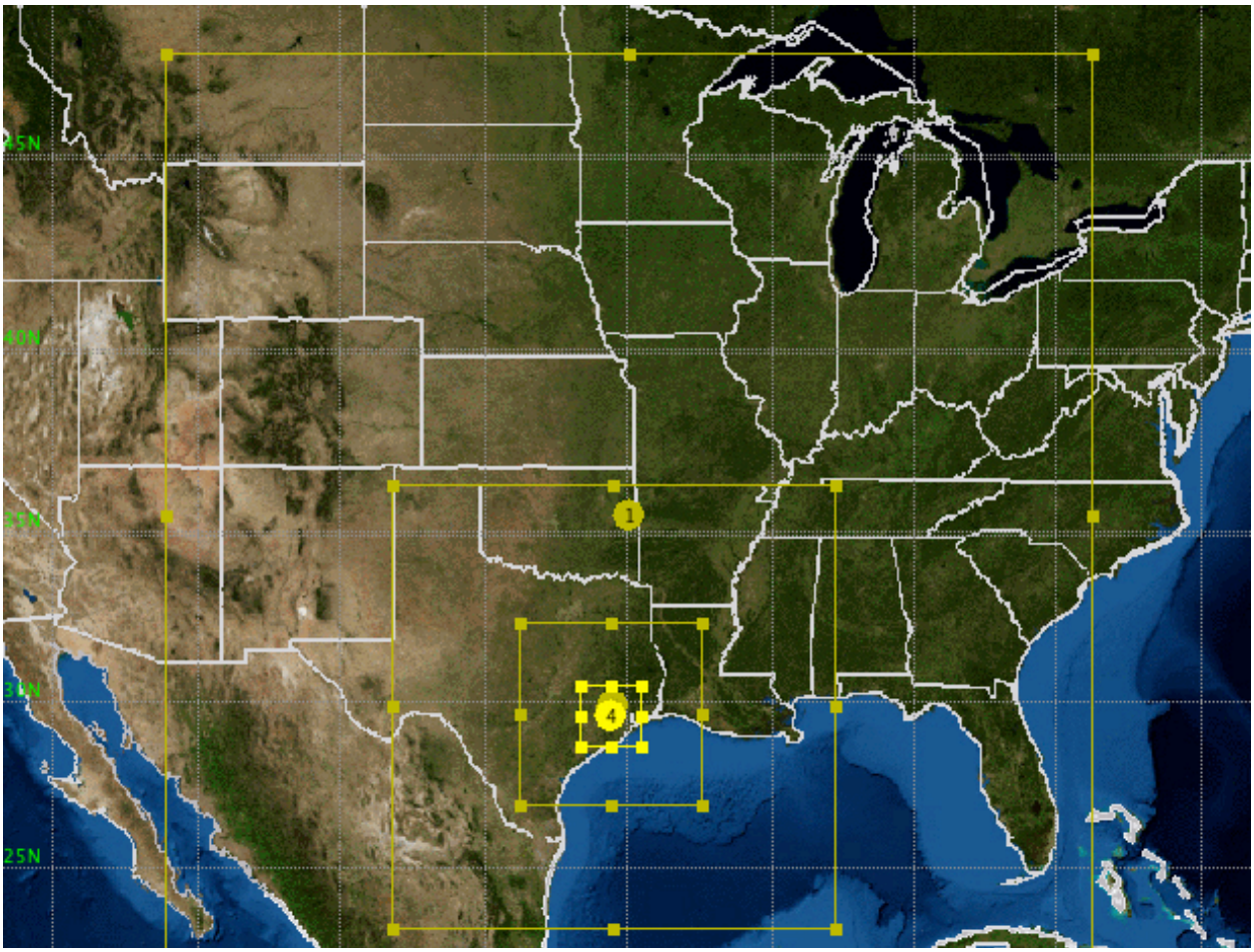

Fig. 3.2. The four WRF model domains for the simulations used herein. The primary study area is the fourth domain.

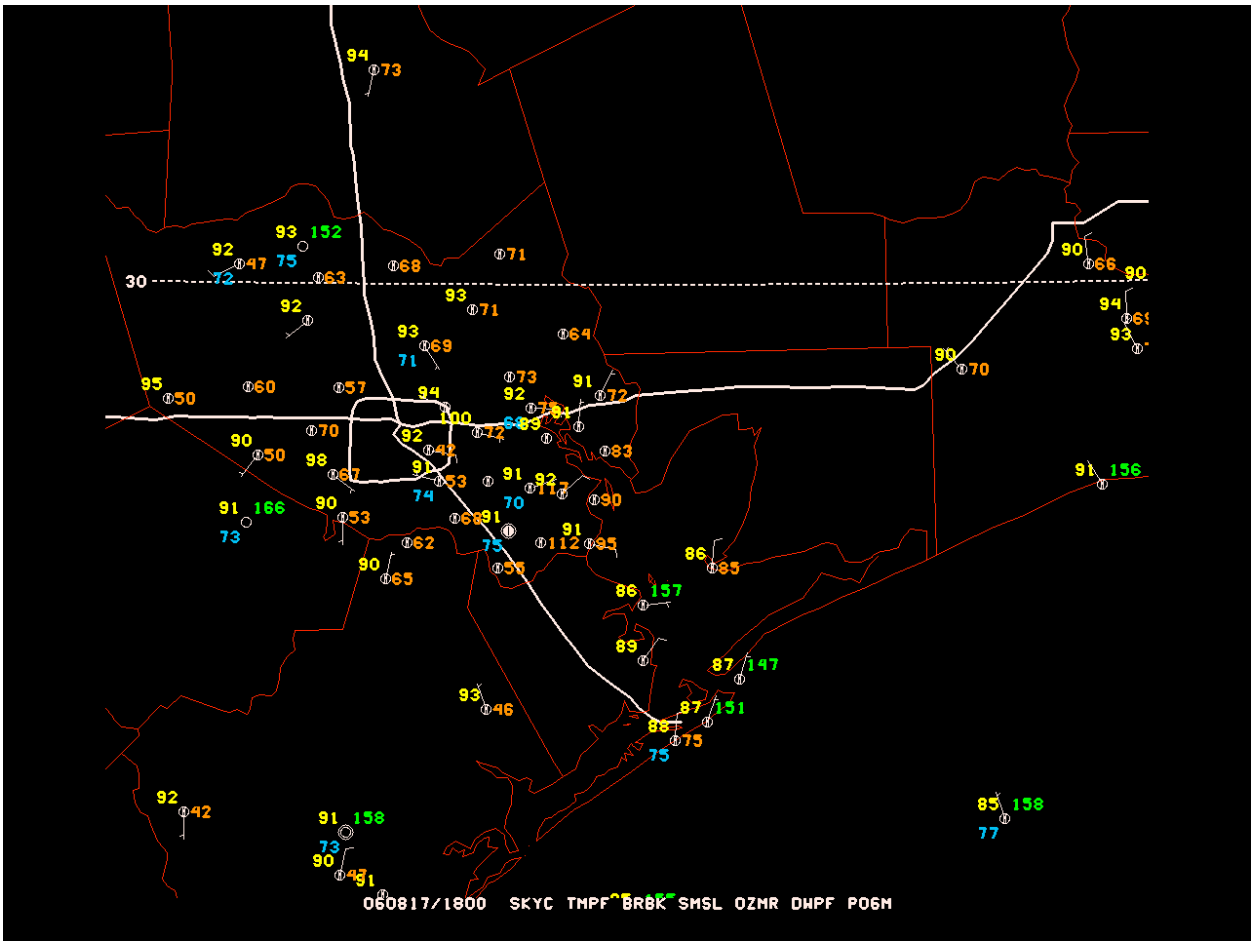

Fig. 3.3. 17 Aug 2006 1800 UTC station plot showing the conditions at and locations of the TexAQS weather stations in the Houston area (from http://atmo.tamu.edu/texaqs2).

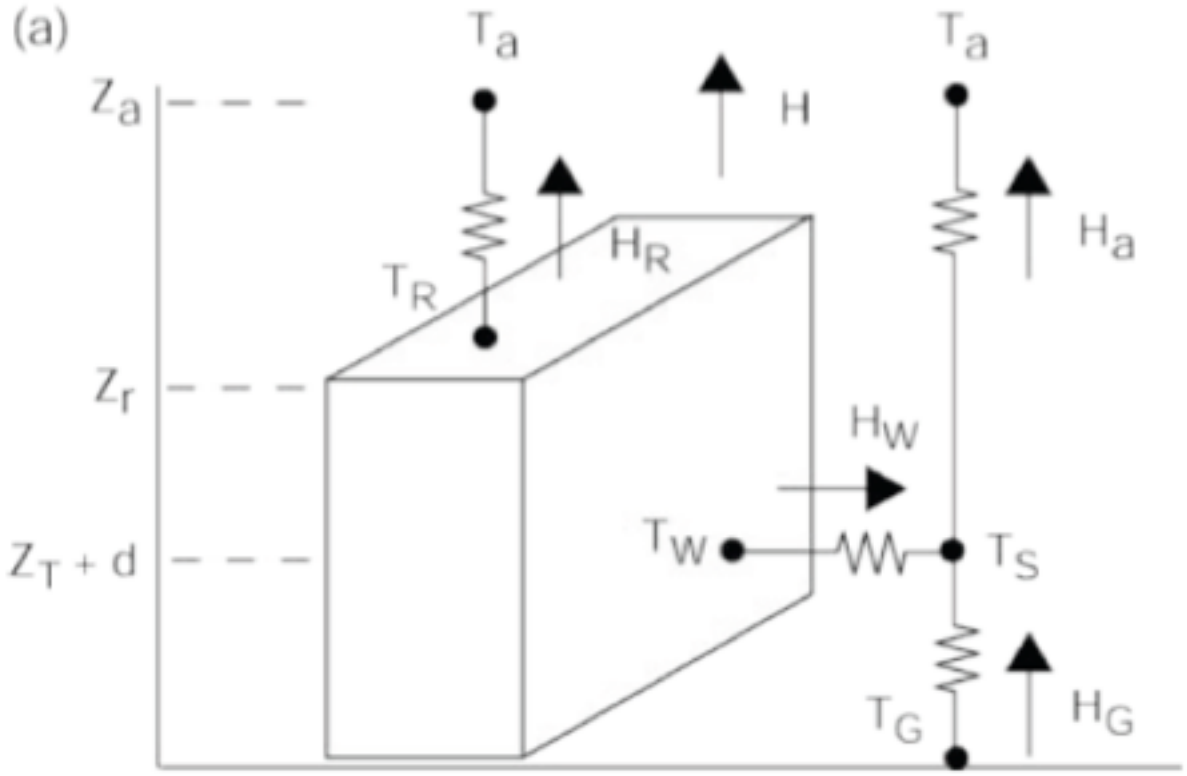

Fig. 3.4. Illustration of components of the WRF Urban Canopy Model. T_a is the air temperature at reference height z_a, T_R is the building roof temperature, T_W is the building wall temperature, T_G is the road temperature, T_S is the temperature defined at $z_T + d$, H is the sensible heat exchange at the reference height, Ha is the sensible heat flux from the canyon space to the atmosphere, H_W is that from wall to the canyon space, H_G is that from road to the canyon space, and H_R is that from roof to the atmosphere (from Chen et al. 2004).

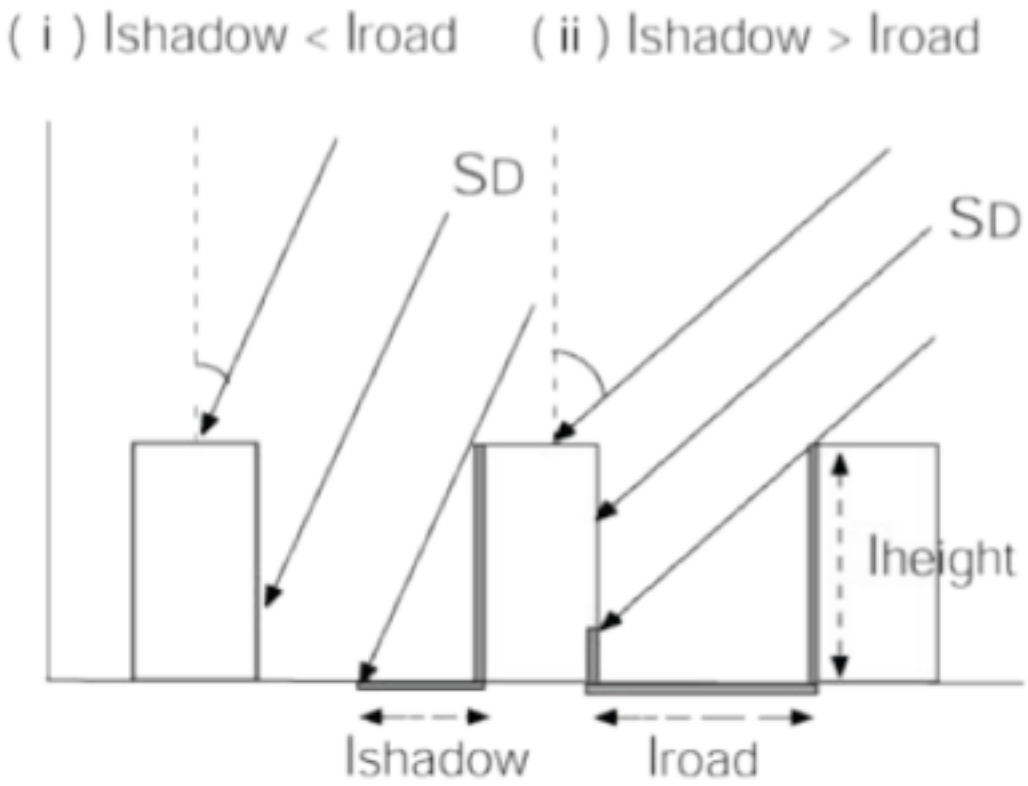

Fig. 3.5. Illustration of the importance of building height and sky view factor within the WRF-UCM. SD is the direct solar radiation incident on a horizontal surface, lroad is the normalized road width, hc is the normalized building height (lroof + lroad = 1), and lshadow is the normalized shadow length on the road (from Chen et al. 2004).

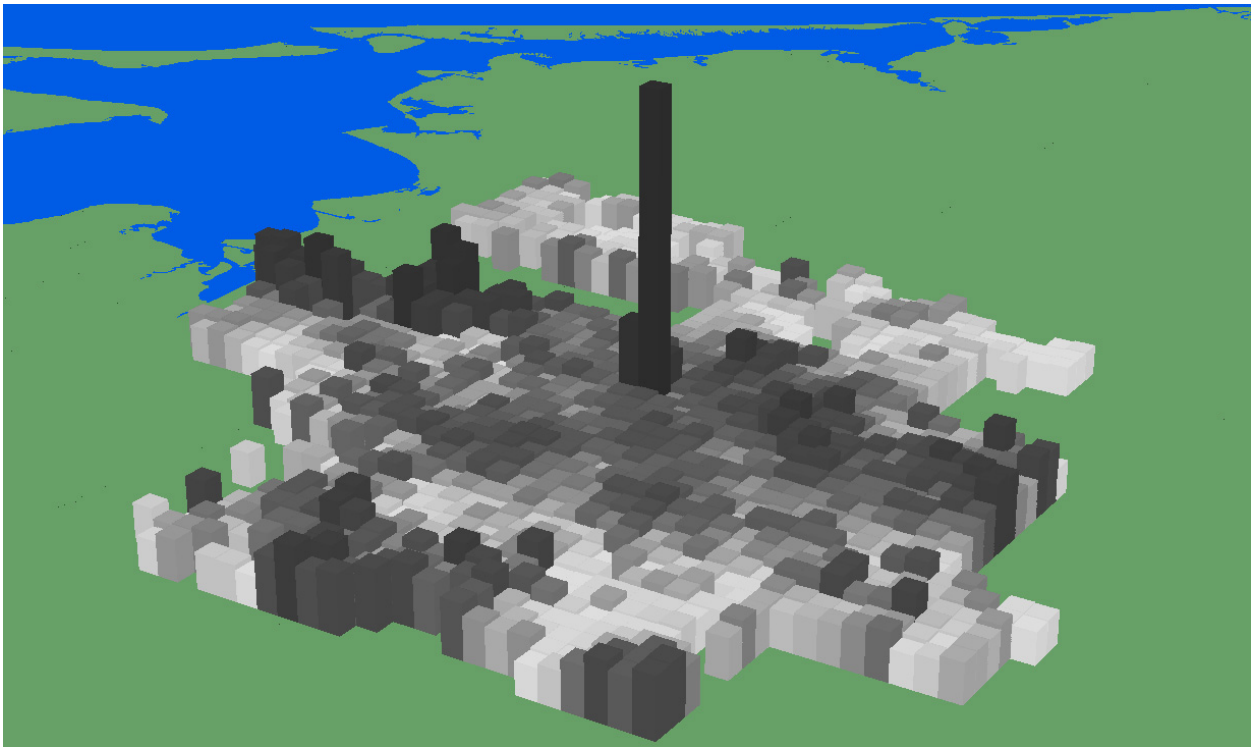

Fig. 3.6. Representation of mean building height from the Burian data set aggregated to model grid resolution.

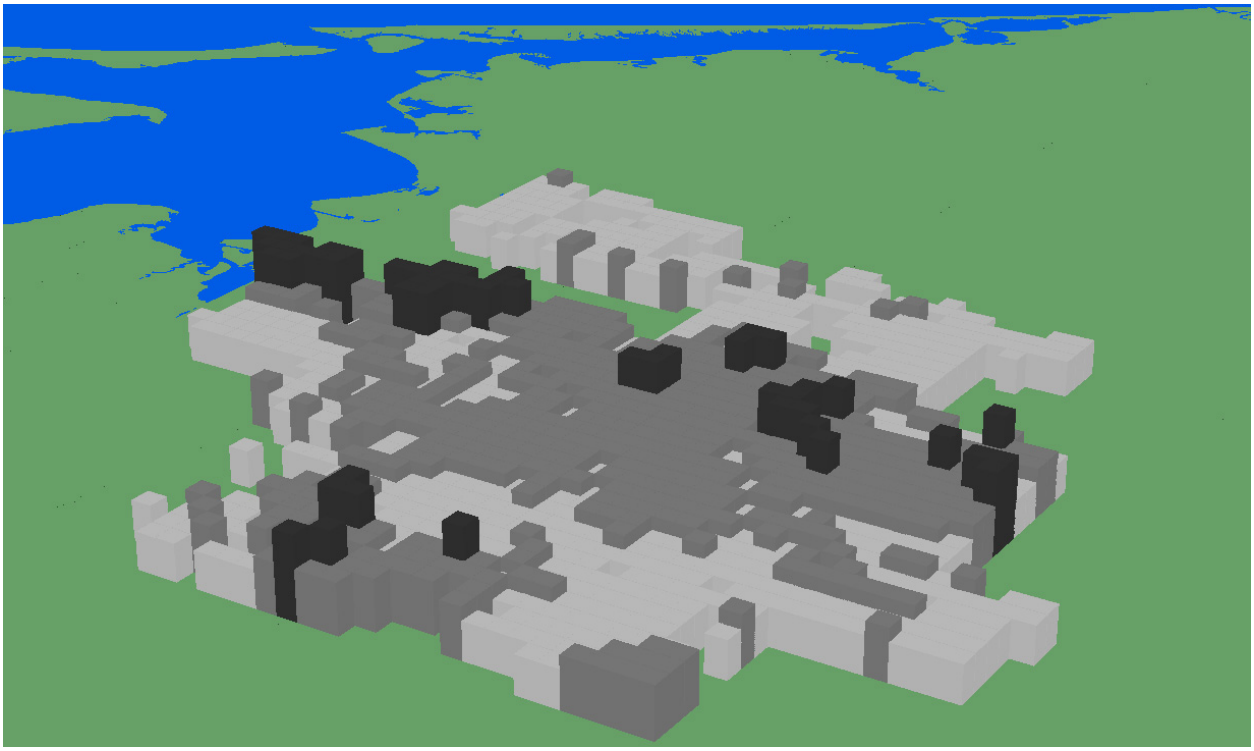

Fig. 3.7. Representation of mean building height of the three aggregated enhanced urban land use categories.

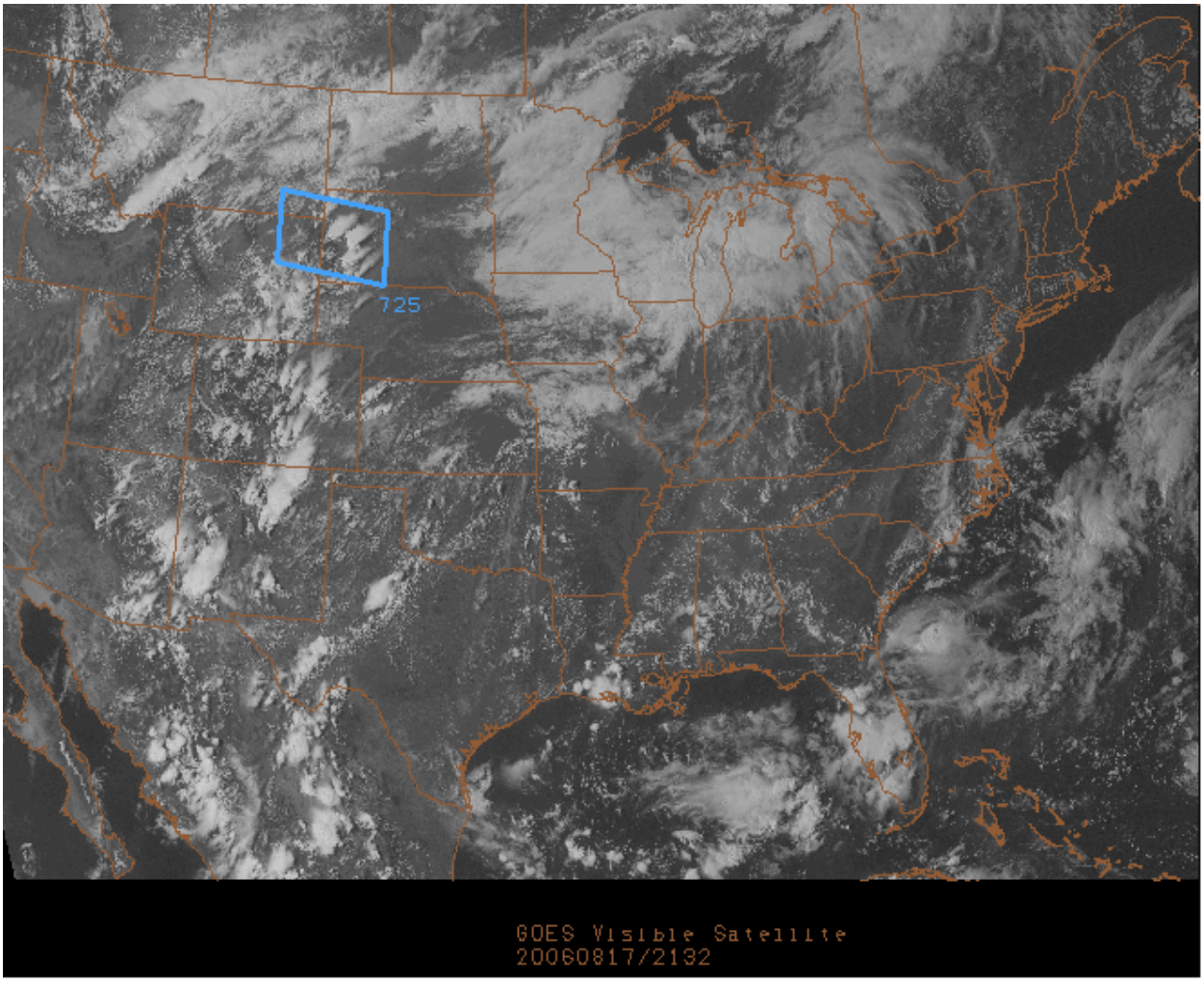

Fig. 3.8. GOES visible satellite image from 2132 UTC, 17 Aug 2008 illustrating environmental conditions during the case period. The blue trapezoid is is not relevant to the study.

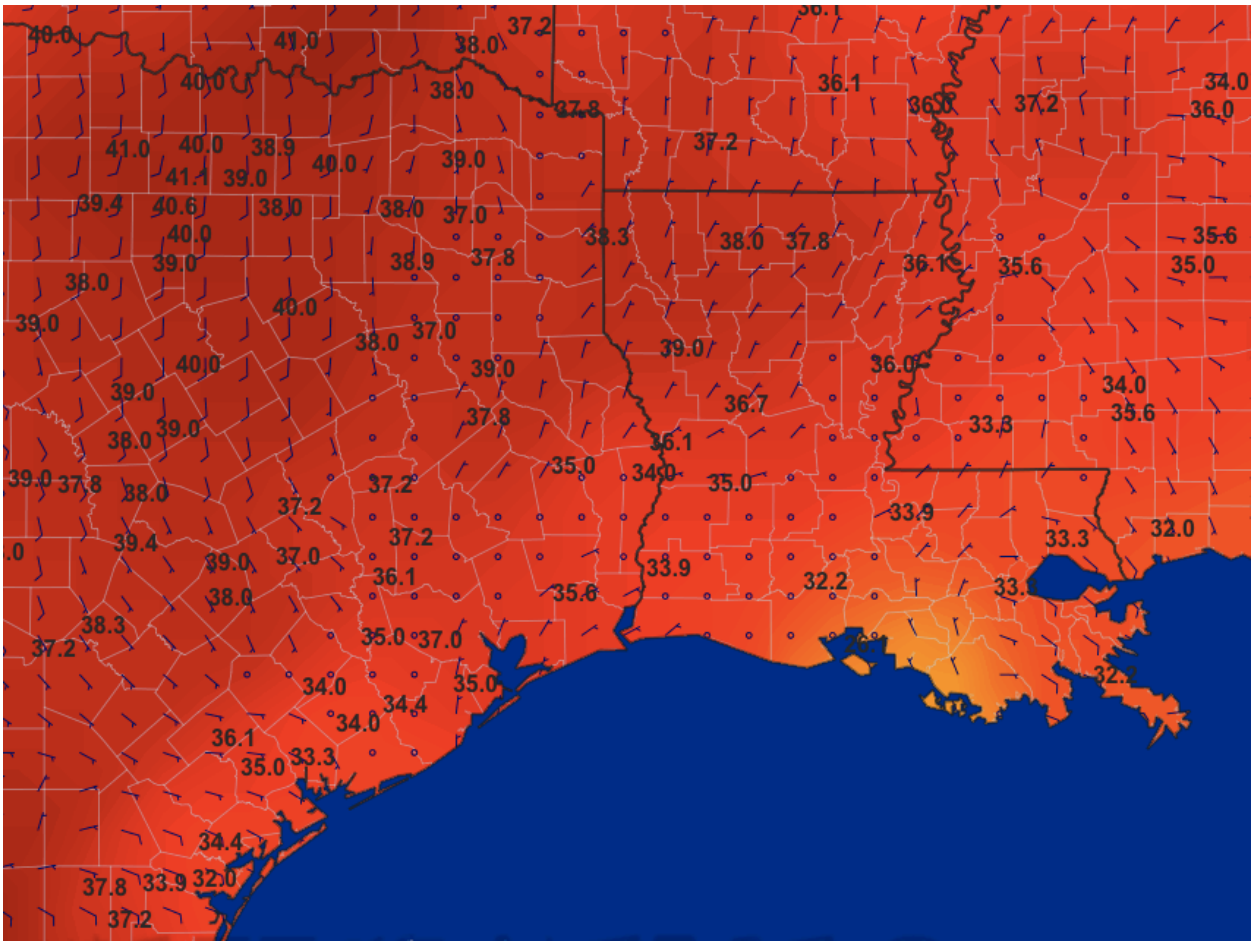

Fig. 3.9. Surface temperature (ºC) and wind barbs from 2100 UTC, 17 Aug 2006 illustrating conditions during the study period (data source, National Weather Service).

CHAPTER 4

RESULTS

4.1 Convective Pump Evolution

The results of the SimpleUrban simulation clearly show the initiation and evolution of a convective pump over the city of Houston during the study period. The theoretical model of the convective pump holds that the vertical motion is initialized by increasing the temperature, and thus reducing the density and increasing the buoyancy of the near surface atmosphere. Fig. 4.1 shows that the SimpleUrban simulation was able to reproduce this initial forcing mechanism, with a persistent skin temperature anomaly over the urban area during the late afternoon and early evening hours. The exact magnitude of the anomaly varies from location to location and from hour to hour, but it approaches 10°C in some areas. It is this skin temperature anomaly which provides the energy to destabilize the lower atmosphere and initiate the convective pump.

Examination of the near surface convergence (plotted as negative divergence) shows that the convective pump begins to initialize around 2100 UTC (1600 CDT) as a series of diffuse disorganized convergence anomalies throughout the urban area. Fig. 4.2 shows that by 2200 UTC (1700 CDT) these anomalies have consolidated into a coherent convective pump structure. The near surface convergence anomaly is strongest during the convective pump's initiation and then begins to slack, suggesting that while the convective pump is formed by surface based mechanisms, it decouples from the surface and begins to lift higher into the atmosphere once it is fully developed.

A clearer picture of the spatial extent and evolution of the convective pump can be seen by examining the BRN shear field. As described previously, the BRN shear value (eqn. 3.1) is the denominator of the BRN equation and can be used to describe the inflow kinetic energy of an updraft, in this case the convective pump. Areas where strong updrafts are occuring are characterized by negative values of BRN shear while stable, nonconvective airmasses exhibit higher values. BRN shear is commonly used to assess severe storm environments, but this application is believed to be novel. It was first applied in work by (Shepherd and Shem, 2009 personal communication) to examine urban effects of tornadic storms around Atlanta. Fig. 4.3 illustrates the evolution of the convective pump from this perspective. The lighter blue areas indicating low BRN shear values inland are likely caused by convective updrafts from daytime heating, such as often results in a field of cumulus humilis clouds. The green, yellow, and red areas denoting higher BRN shear values are those where the stable, marine airmass has begun to intrude. Thus, by using this metric, the evolution of the convective pump and its interaction with the sea breeze airmass can be shown. As described previously, the convective pump begins as a series of diffuse, disorganized convective anomalies over the urban area at 2100 UTC (1600 CDT). By 2200 UTC (1700 CDT) the convective pump has become more organized and by 2300 UTC (1800 CDT) it is completely developed. By 0000 UTC (1800 CDT) the marine airmass has begun to encroach on the southern fringes of the urban area and by 0100 UTC (1900 CDT) it has penetrated deeply enough into the city to begin to displace the convective pump to the north. At 0200 UTC (2000 CDT) the convective pump has been completely displaced to the north of the city, and has both weakend and become smaller in extent due to being removed from its energy source, the elevated near surface temperatures of the urban area.

Furthermore, through the use of these simulations, it is possible to show that the convective pump is entirely caused by the presence of the urban environment. Fig. 4.4 shows the results of subtracting the skin temperature from the NoUrban simulation, in which the entire urban area is removed and replaced with cropland, with the SimpleUrban simulation. The result shows that there is a skin temperature anomaly of 7-8°C caused solely by the presence of the urban environment at 0000 UTC (1800 CDT) when the convective pump is fully mature. The same technique can be applied to the BRN shear field, the results of which are shown in Fig. 4.5. An anomaly of lower BRN shear values can be seen both over and to the north of the city, confirming that the convective pump is indeed urban induced. The positive BRN anomaly to the west of the city is due to the difference in sea breeze front morphology caused by interaction with the urban area which will be discussed in the next section.

4.2 Sea Breeze Morphology

The SimpleUrban simulation was able to reproduce a realistic sea breeze event, allowing for the characterization of the interactions between the sea breeze and urban environment. Fig. 4.6, showing the 2m shelter height temperature and wind speed, summarizes the evolution of the sea breeze in this simulation. At 1900 UTC (1400 CDT) the 2m air temperature over the ocean is cooler than over land, on the order of 4-5°C. By 2100 UTC (1600 CDT), the sea breeze has begun to set up, and the marine airmass begins to intrude inland, creating a sharp mesoscale temperature gradient. At 2300 UTC (1800 CDT) the sea breeze has begun to interact with the southern extent of the urban area, and by 0100 UTC (2000 CDT), the marine airmass has begun to bifurcate around the urban heat island. By 0300 UTC (2200 CDT) the sea breeze has

completely split around the urban heat island, which has itself begun to advect northward. At 0500 UTC (0000 CDT), the sea breeze has completely overwhelmed the city, though an urban heat island signature remains.

At the forward extent of the maritime airmass, the intrusion of cooler, stable air lifts the warmer inland airmass, similar to a synoptic scale cold front or mesoscale outflow boundary. This lifting results in a vertical motion anomaly, known as the sea breeze front, which can be characterized using the near surface vertical velocity field from the SimpleUrban simulation, as shown in Fig. 4.7. At 1900 UTC (1400 CDT), the boundary lies along and parallel to the coast. The role of coastal morphology in generating sea breeze front structures can already be seen, particularly in the enhancement of the sea breeze front inland of the convex coastline near Smith Point on the eastern side of Galveston Bay. The noisy signal inland is a result of convective updrafts from diurnal heating leading to the formation of a cumulus field, as discussed earlier. By 2100 UTC, (1600 CDT) the boundary has begun to push inland, and further enhanced areas of vertical motion can be seen, again primarily near areas where the coastline is convex. Also of note at this time is that vertical velocity are anomalies beginning to form over the city as the convective pump begins to initiate. At 2300 UTC (1800 CDT) the complex structures of the fully mature sea breeze front are evident, including a series of vertical velocity anomalies perpenidicular to the coast where the sea breeze front has folded in on itself. By 0100 UTC (2000 CDT) the diurnal cumulus field has collapsed, and the sea breeze front has penetrated the core of the urban area and combined with the convective pump vertical velocity anomaly. At 0300 UTC (2200 CDT), the combined urban-coastal anomaly has been translated to the north of the city while the sea breeze boundary has become mostly diffuse, except to the west of the city. At 0500

UTC (0000 CDT) the original sea breeze boundary has completely dissipated, and a new boundary is beginning to set up near the coast due to the land breeze.

One of the primary goals of this study is to understand the role of urbanization on the evolution of the sea breeze front, and to show how sea breeze front structures are altered due to their interaction with the urban area, as opposed to the patterns which develop solely due to coastal morphology. This is achieved by again performing a differencing analysis, this time by subtracting the NoUrban near surface vertical velocity field from the SimpleUrban vertical velocity field. The result is shown in Fig. 4.8. The position of the sea breeze front in the SimpleUrban scenario is indicated by darker colors in the vertcial velocity field. The position of the boundary in the NoUrban scenario is indicated by lighter colors. Where the field is neutral (medium blue) this indicates that the urban area had no effect on the sea breeze boundary, and any structures which developed were purely a function of coastal morphology. It is clear that, through its interaction with the urban-induced circulation, the sea breeze boundary is both strengthened and accelerated in its inland progress, similar to the findings of Ohashi and Kida (2002). This has the effect of reducing the dwell time of the sea breeze front over the urban area, while simultaneously increasing the strength of the vertical velocity anomaly. At 0100 UTC (2000 CDT), the NoUrban boundary lags behind the SimpleUrban boundary on the western edge of the city by as much as 10-15km. The SimpleUrban boundary continues to surge ahead of the NoUrban boundary until 0300 UTC (2200 CDT) when the sea breeze front has begun to pass the urban area, and the acceleration of the boundary due to urban influences has slowed. Also at this time, a combined urban-coastal vertical velocity anomaly has developed on the northern edge of the city, coincident with the northern advection of the convective pump discussed earlier. By

0330 UTC (2230 CDT CDT) the SimpleUrban and NoUrban boundaries have synchronized, indicating that the presence of the city does enhance and accelerate the sea breeze front while it is interacting with the urban area similar to the findings of Lo et al. (2007) in the Pearl River Delta of China. In the case of Houston however the city does not cause the sea breeze front to penetrate further inland than in would if the it were not present.

4.3 Combined Urban-Coastal Circulations in the SimpleUrban Scenario

The combined evoloution of urban-coastal circulations can be characterized by a series of vertical cross sections taken through the urban area (Fig. 4.9). Results indicate that the evolution of urban-coastal circulations can be described as proceeding through four stages (Fig. 4.10). A conceptual illustration of these stages is shown in Fig. 4.11. In Stage 1, occurring in the early afternoon, the differential heating of the urban land surface creates an "urban heat bubble" which acts as a barrier to the environmental wind. This leads to convergence on the perimter of the urban area and an associated vertical velocity anomaly. Shem and Shepherd (2009) and Shepherd et al. (2009) have also observed increased convergence along the inner periphery of urban land footprint. Stage 2 is the initiation of the convective pump, which occurs in the mid-afternoon. The increasingly warm lower atmosphere within the city boundaries becomes unstable, and a series of small convective structures develop, which slowly consolidate into a coherent convective pump. Stage 3 is characterized by the penetration of the sea breeze front into the urban area in the early evening, which combines with the convective pump to generate a strong vertical velocity anomaly which progresses through the city from south to north. Finally in Stage 4, which occurs in the late evening through the early morning hours, the stable maritime airmass

has completely overwhelmed the urban area and wind vectors below 900 hPa have taken on a substantial southerly component.

4.4 Sensitivity to Enhanced Urban Canopy Parameters

A secondary goal of this study was to evaluate the sensitivity of WRF-ARW simulations to the inclusion of enhanced urban canopy parameters. This is done by creating an enhanced UCP land cover data set as decribed previously. The enhancements to this data set are shown in Fig. 4.12. Fig. 4.13 shows the results of including this enhanced land cover on skin temperature. While early in the afternoon the differences are mainly confined to areas where the enhanced land cover is signifcantly different from the SimpleUrban land cover, by 2100 UTC (1600 CDT) the enhanced UCPs have led to a very complex surface thermal structure. In order to evaluate the use of these UCPs, the results of the UCPUrban and SimpleUrban simulations were compared to observations from the study area. Five sites were chosen (Fig. 4.14) from the TexAQS data set to represent the different land covers within the Houston area. Time series of 2m temperature were plotted for each location and for the equivalent location within the two simulations (Fig. 4.15). An impact score was calculated for each site based on the root mean square error of the bias between the observed and predicted temperatures (Table 4.1):

Table 4.1. Impact score describing the improvement to representation of 2m air temperature casued by the inclusion of enhanced urban canopy parameters. Larger values indicate reduced bias with respect to ground observations.

Aldine	Wharton	Houston Reg.	Houston East	Bayland
0.082	-0.027	0.009	0.093	0.019

A positive impact score indicates that the enhanced UCPs improved the representation of 2m temperature relative to the SimpleUrban simulation. For example, in the case of Houston East, the enhanced UCPs reduced bias by 9.3% of a standard deviation. It appears that the UCP data has the largest positive impact on areas that have significantly higher or lower urban density than average, such as Aldine, which is in a suburban area far from the central business district, and Houston East, which is located near the highly industrial Ship Channel. Areas of moderate urban density, such as Houston Regional and Bayland, exhibit little improvement due to the inclusion of enhanced UCPs, likely becasue they were already well represented by the SimpleUrban urban characteristics. The only site that showed a detrimental effect from the inclusion of enhanced UCPs was Wharton, indicating that it may be miscategorized in the enhanced UCP data set or that sub model-scale effects may play an increased role in temperature evolution at this site.

Understanding the implications of enhanced urban canopy parameters on the evolution of urban-coastal circulations and on atmospheric transport was also of interest for this study. Analysis of the BRN shear difference between the UCPUrban and SimpleUrban simulations shows that the primary impact of enhanced UCPs on the evolution of the convective pump occurs early in its development, around 2100 UTC (1600 CDT) (Fig. 4.16). In general, this fits

well with the conceptual model for the evolution of the convective pump outlined previously, which states that once the convective pump becomes mature, it decouples from the surface where the enhanced UCPs would have the greatest impact. Futhermore, the impact of enhanced urban canopy parameters is not limited to the urban environment itself. Fig. 4.17 shows the difference in vertical velocity caused by the inclusion of the enhanced UCPs. While early in the afternoon the vertical velocity perturbations are mostly limited to areas within the urban boundaries, these perturbations quickly begin to propagate westward into the surrounding areas. This westward propagation of vertical velocity anomalies is of particuar interest since it has already been shown that the primary impact of the urban area on the evolution of the sea breeze front was to the west of the city.

Finally, to address the issue of transport, a series of parcel trajectories were plotted (Fig. 4.18). These trajectories simulate the path of a series of parcels released along a southwest to northeast transect through the urban core and surrounding areas at 2100 UTC (1600 CDT) and allowed to advect for four hours. The “chimney effect” of the convective pump is clearly visible, as parcels released from within the urban boundary are drawn upward into the convective pump and reach a greater altitude than those released outside the city. The effect of the urban area on the atmosphere to the west of the city is evident as well, as those parcels follow a similar trajectory as those released within the city, but do not reach as great an altitude, due to the lack of convective pump forcing. Conversely, parcels released to the northeast of the city where the urban impact is minimized remain primarily near the surface and move with the environmental wind.

4.5 Combined Urban-Coastal Circulations in the UCPUrban Scenario

The effect of the inclusion of enhanced urban canopy parameters on urban-coastal circulations can be seen by plotting a series of vertical cross sections as before (Fig. 4.19). The primary difference in evolution occurs in Stage 2, the initiation of the convective pump. The more heterogenous land surface characteristics of the UCPUrban simulation lead to a more complex series of vertical motion anomalies, both positive and negative, which is expected given the higher detail in surface temperature that the UCPUrban simulation is able to resolve. This may have important implications for pollutant transport, as areas where the urban density is overstated by the SimpleUrban scenario may in fact be not convective but subsident. In other words, the convective pump may be stronger over the dense industrial areas where more pollutants are generated, causing greater uptake of pollutants into the atmosphere, while subsident regimes over the suburban areas, where there is lower urban density, may actually lead to increased pollutant transport to these locations.

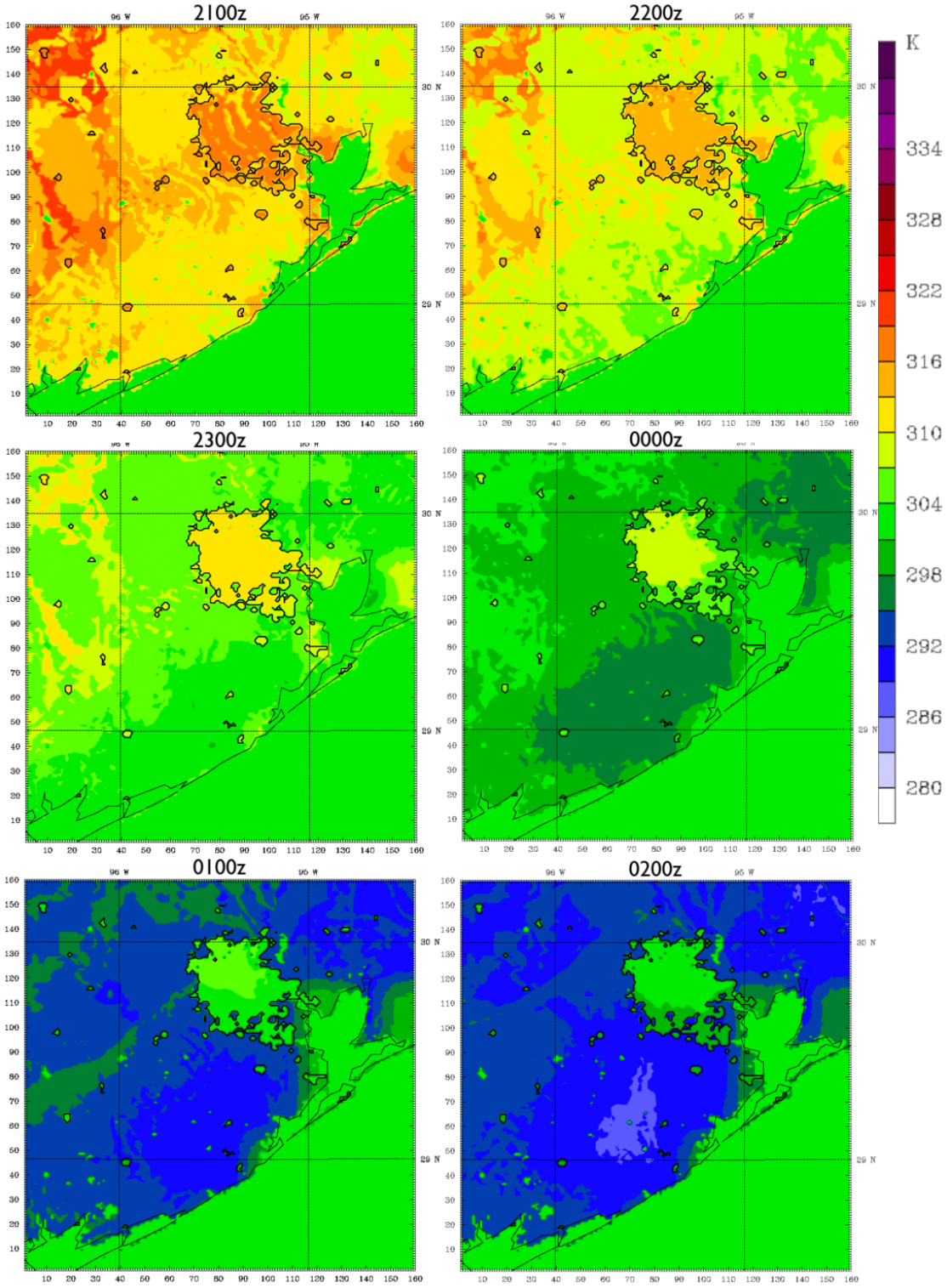

Fig. 4.1. SimpleUrban skin temperature (K) from 2100 – 0200 UTC (1600 – 2100 CDT) showing the persistent skin temperature anomaly over the urban area.

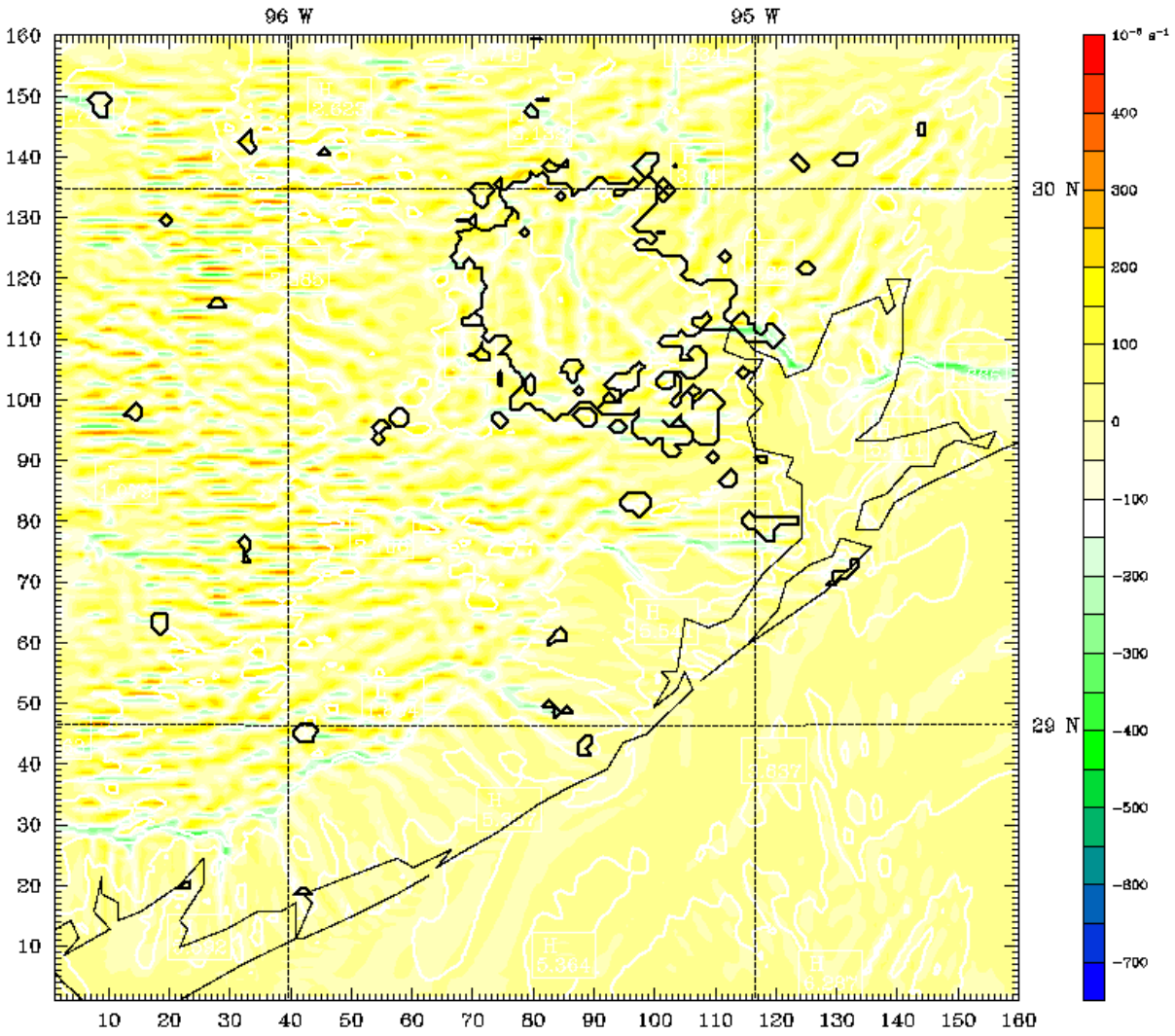

Fig. 4.2. Divergence/convergence field ($10^{-5}s^{-1}$) at 2200 UTC (1700 CDT) showing the convergence anomaly over the urban area associated with the initiation of the convective pump.

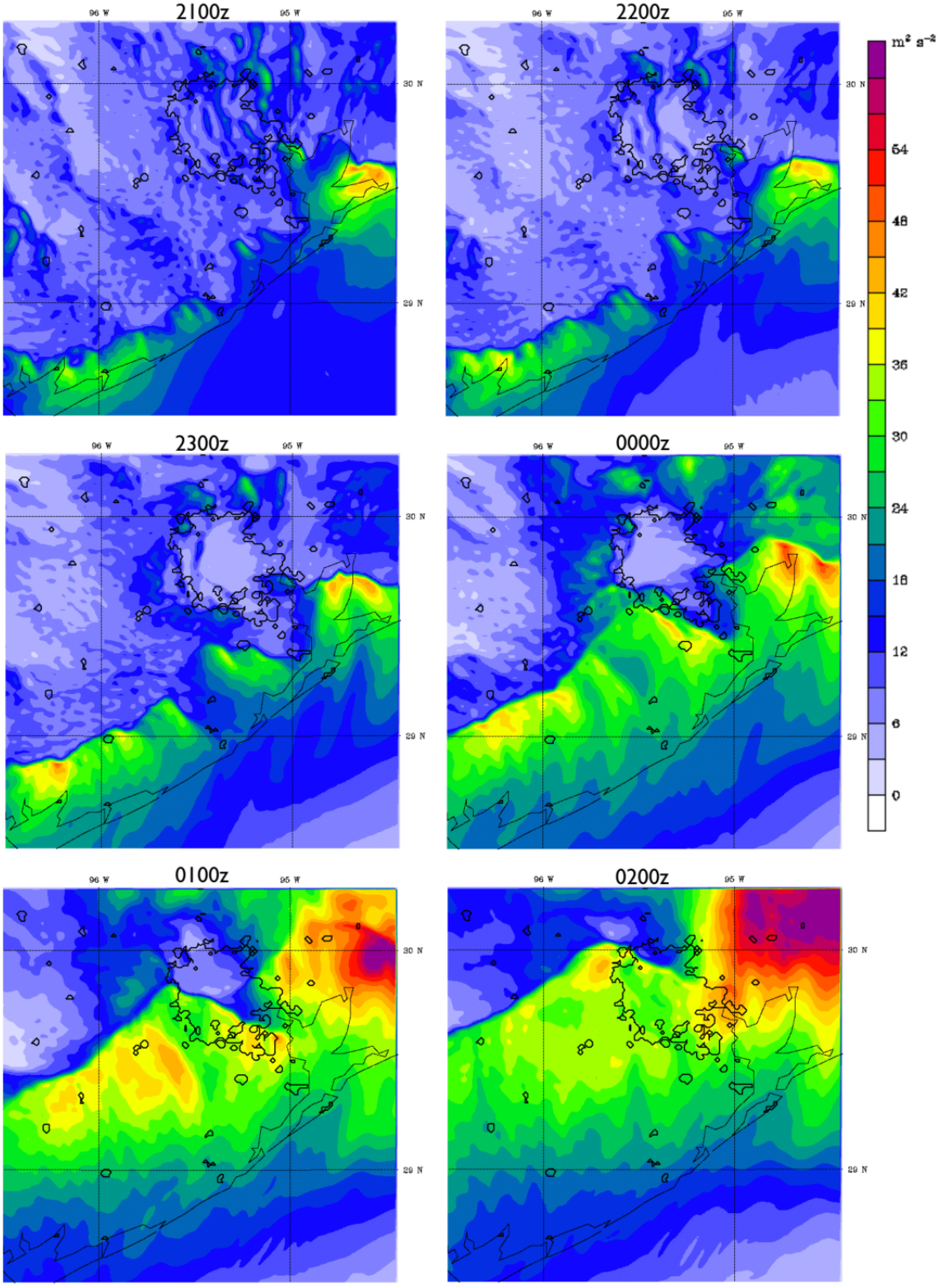

Fig. 4.3. BRN shear field (m^{-2} s^{-2}) 2100 UTC – 0200 UTC (1600 – 2100 CDT) showing the evolution of the convective pump.

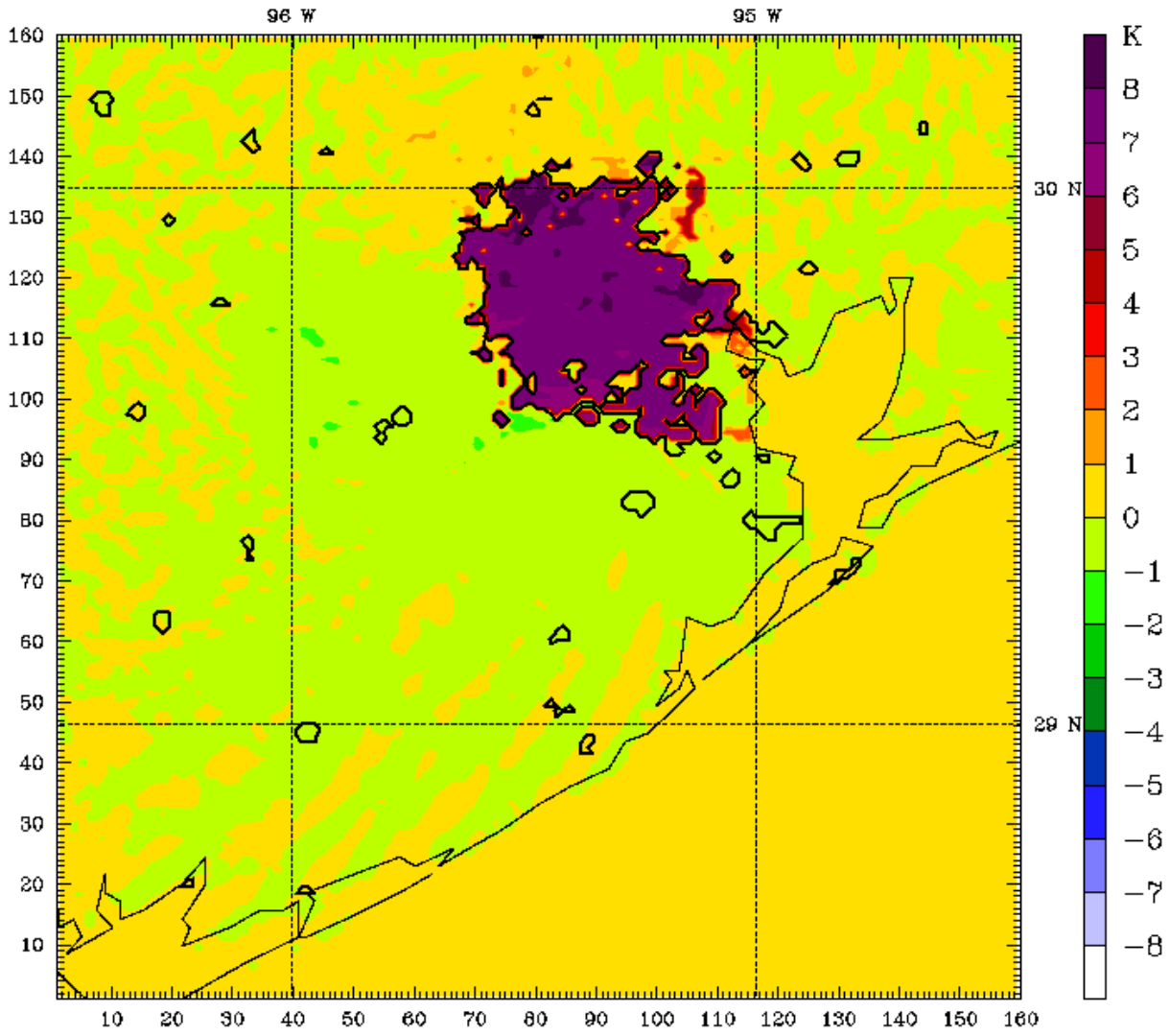

Fig. 4.4. Difference field resulting from the subtraction of the NoUrban skin temperature from the SimpleUrban skin temperature (K) at 0000 UTC (1800 CDT). The urban area is generating a skin temperature anomaly of 7 to 8K.

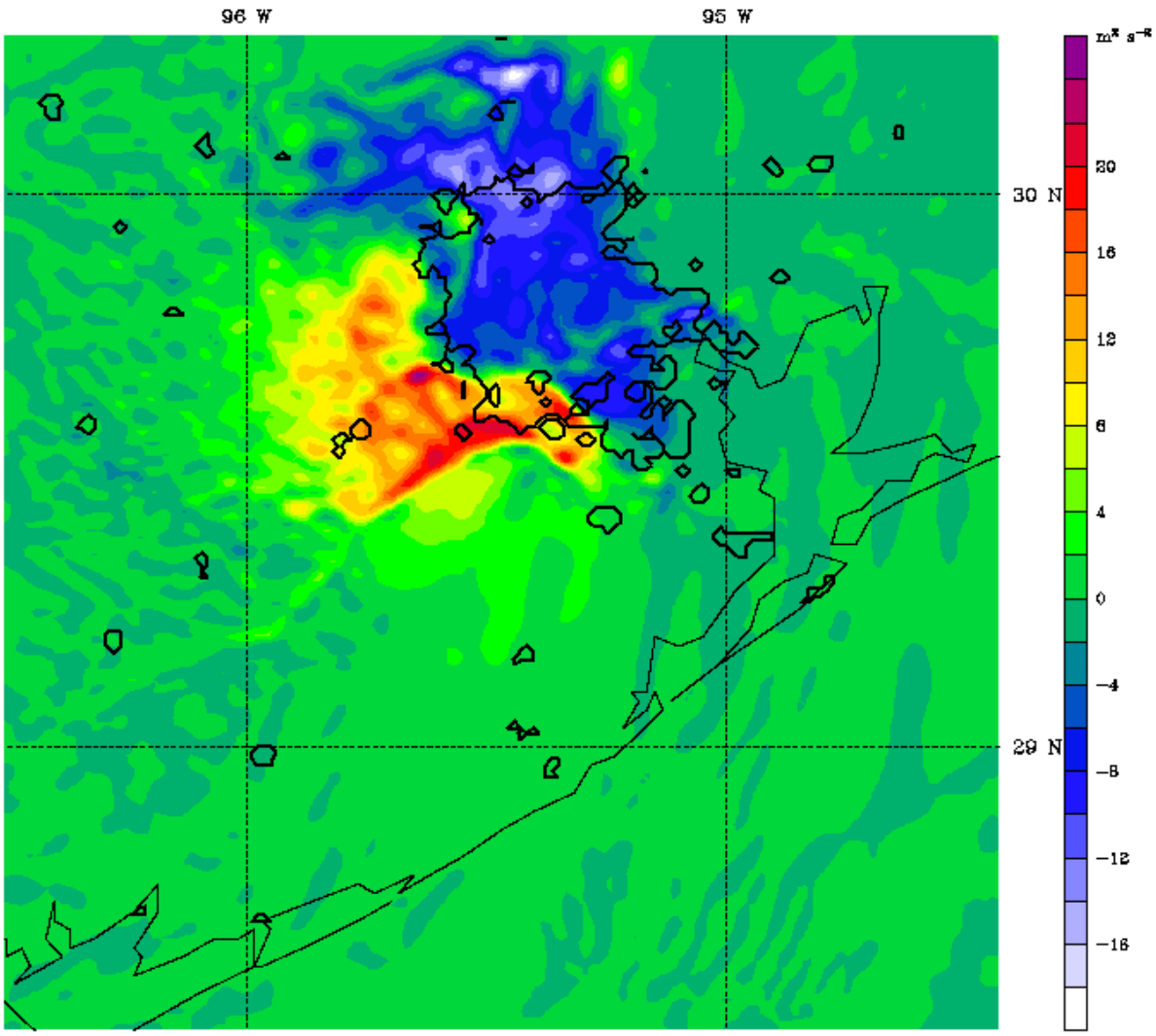

Fig. 4.5. Difference field resulting from the subtraction of the NoUrban BRN shear from the SimpleUrban BRN shear (m^{-2} s^{-2}) at 0000 UTC (1800 CDT). The negative BRN shear anomaly is caused primarily by the presence of the urban area in these simulations.

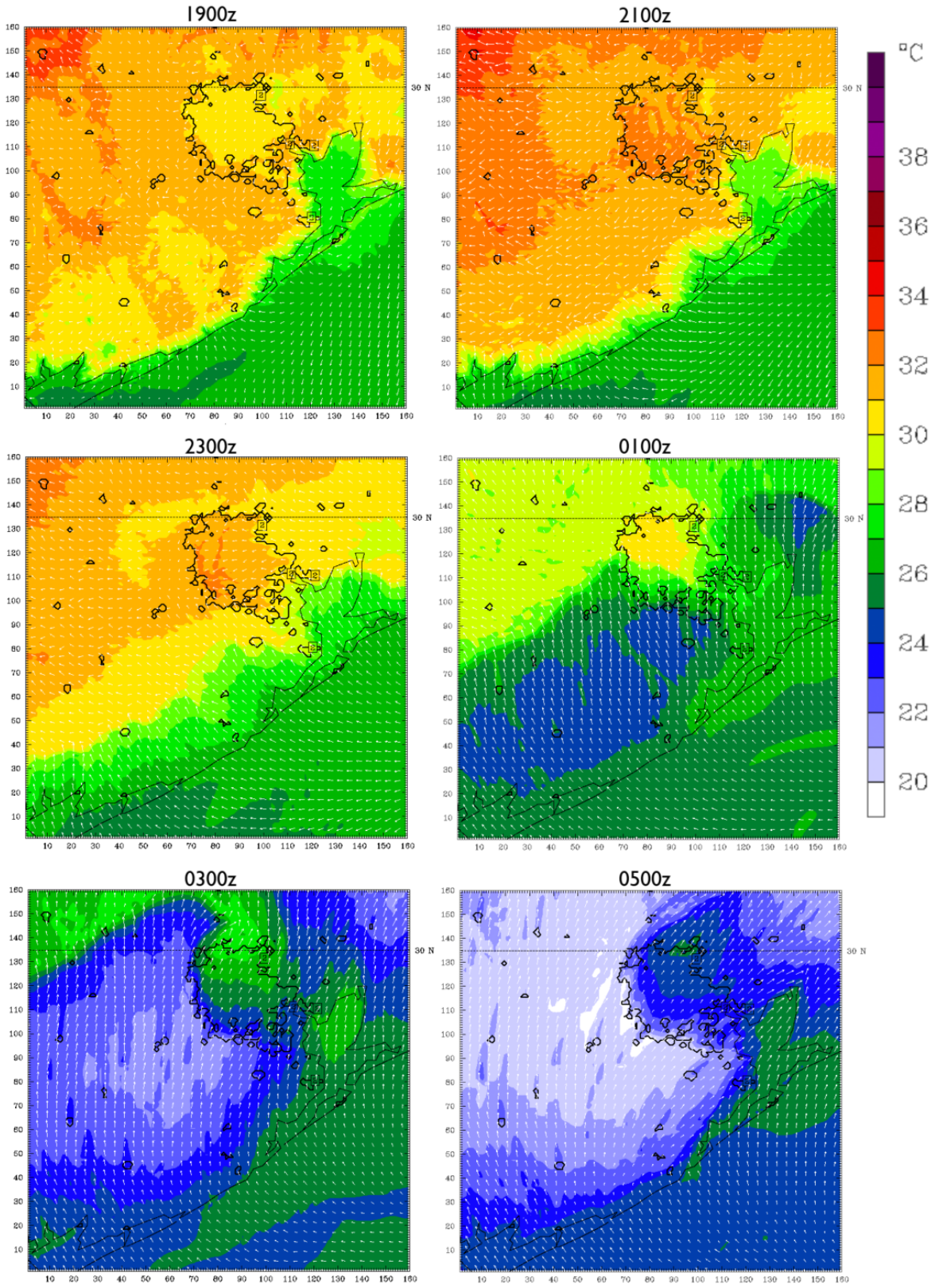

Fig. 4.6. 2 meter air temperature (ºC) and wind direction from 1900 UTC – 0500 UTC (1400 – 0000 CDT) showing the development of the sea breeze and intrusion of the marine airmass.

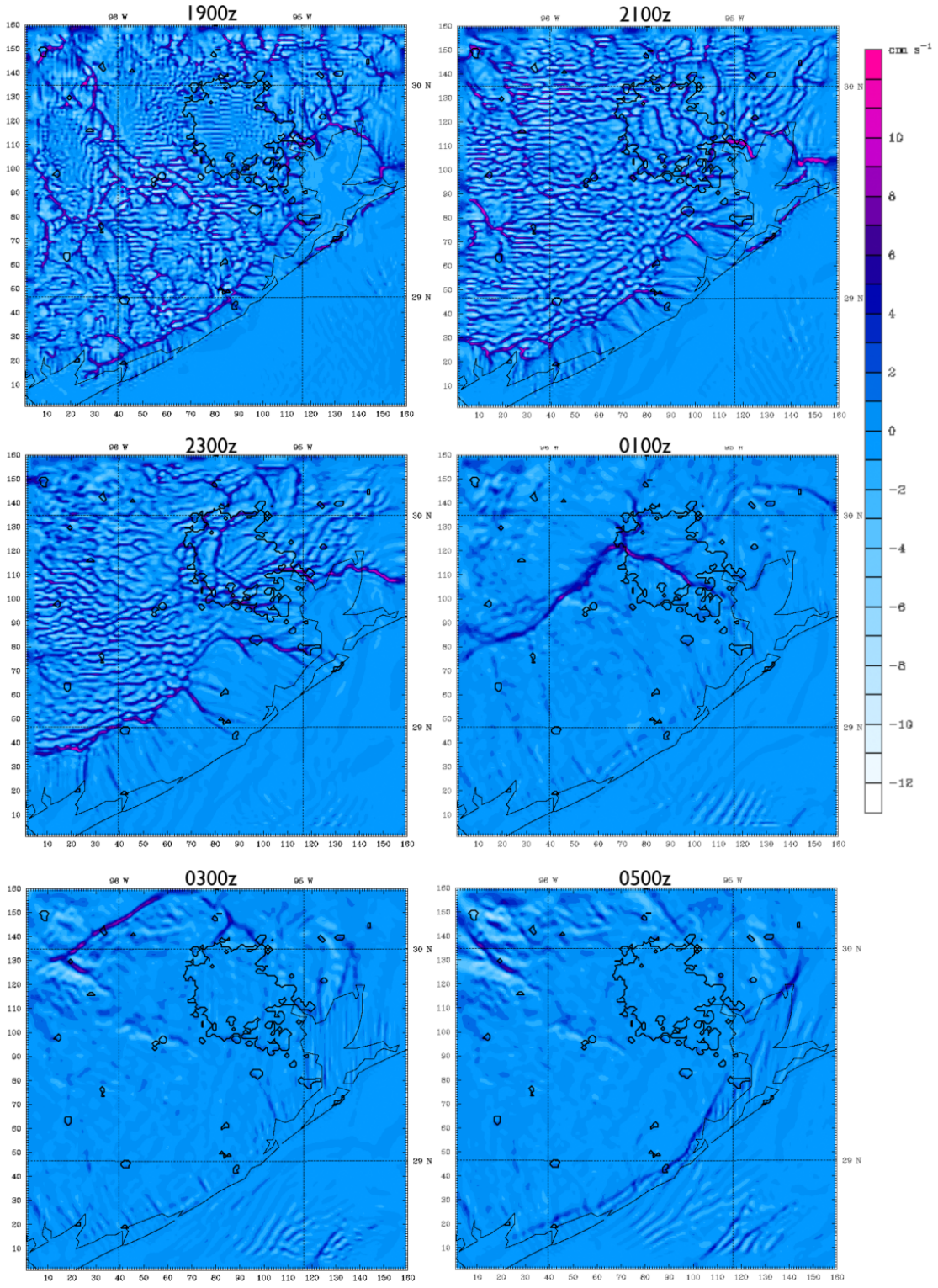

Fig. 4.7. Near surface vertical velocity (cm s^{-1}) from 1900 UTC – 0500 UTC (1400 – 0000 CDT) showing the structure and evolution of the sea breeze front and its interactions with the urban-induced vertical motion associated with the convective pump.

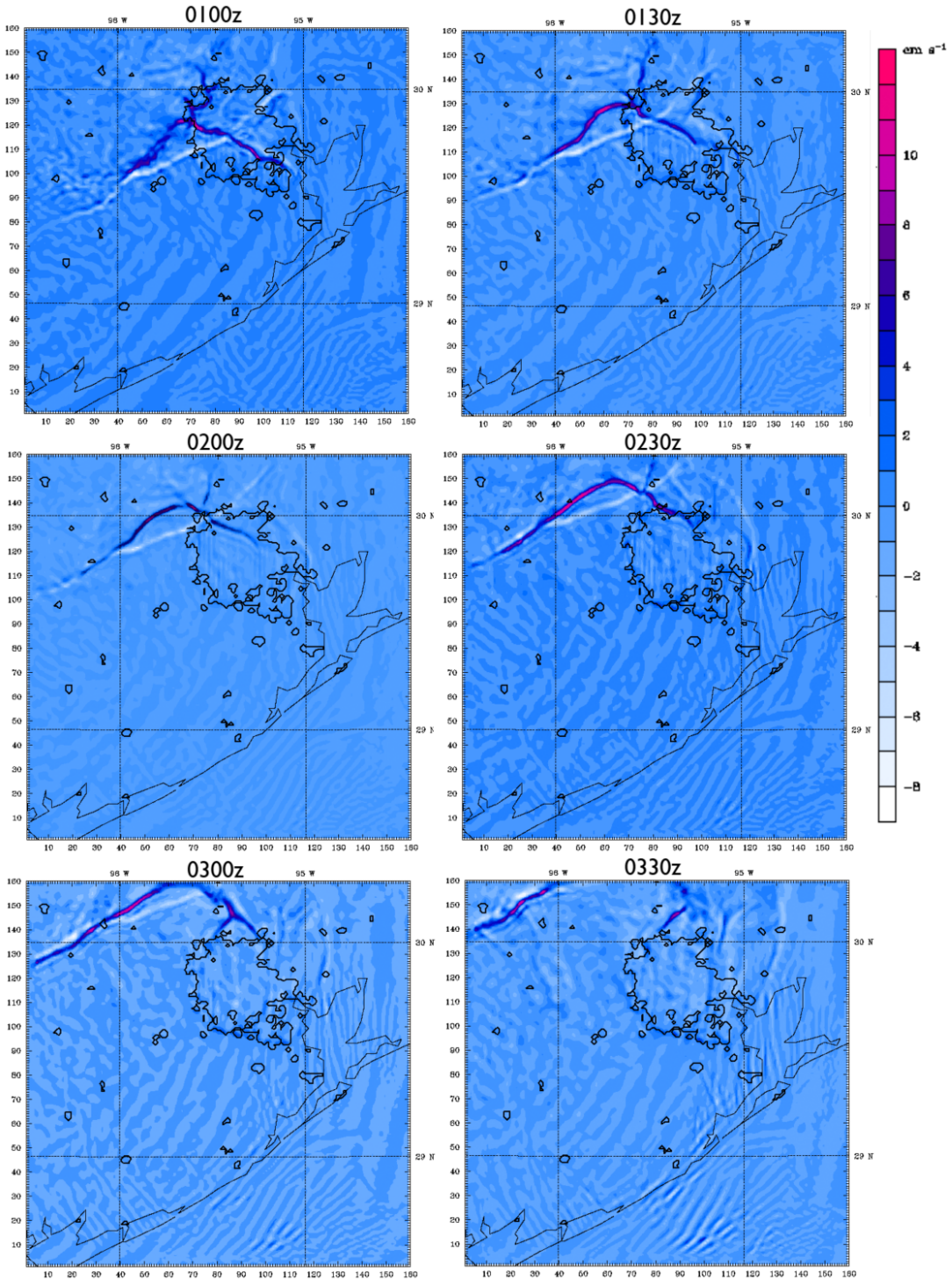

Fig. 4.8. Difference field resulting from the subtraction of the NoUrban near surface vertical velocity from the SimpleUrban vertical velocity (cm s^{-1}) from 0100 UTC – 0330 UTC (2000 – 2230 CDT) illustrating the changes in sea breeze front morphology caused by the presence of the urban area in these simulations. The light colored boundary indicates the position of the NoUrban SBF while the dark colored boundary indicates the position of the SimpleUrban SBF.

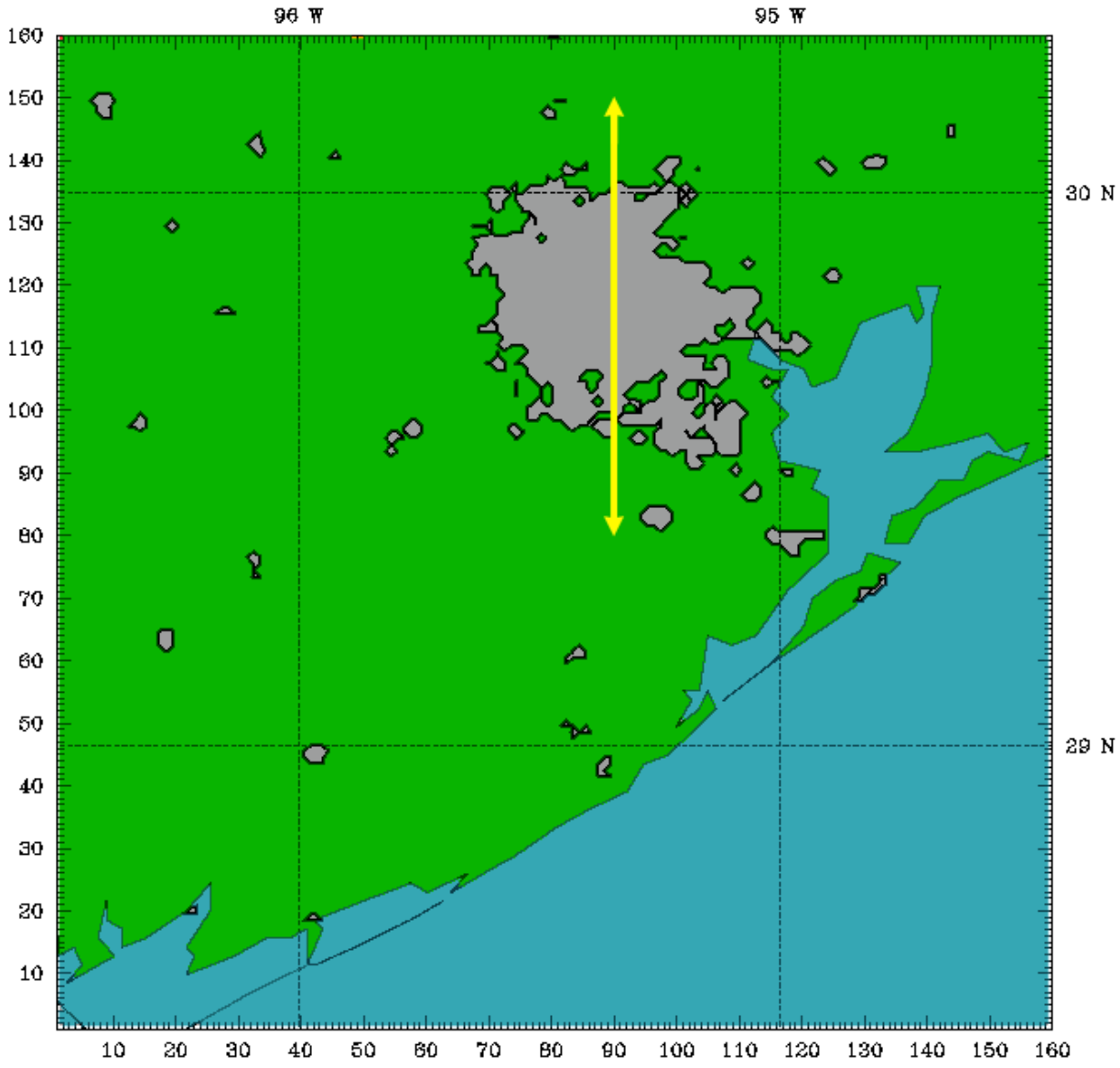

Fig. 4.9. Map of the study area indicating the position of the north to south cross section shown in following figures.

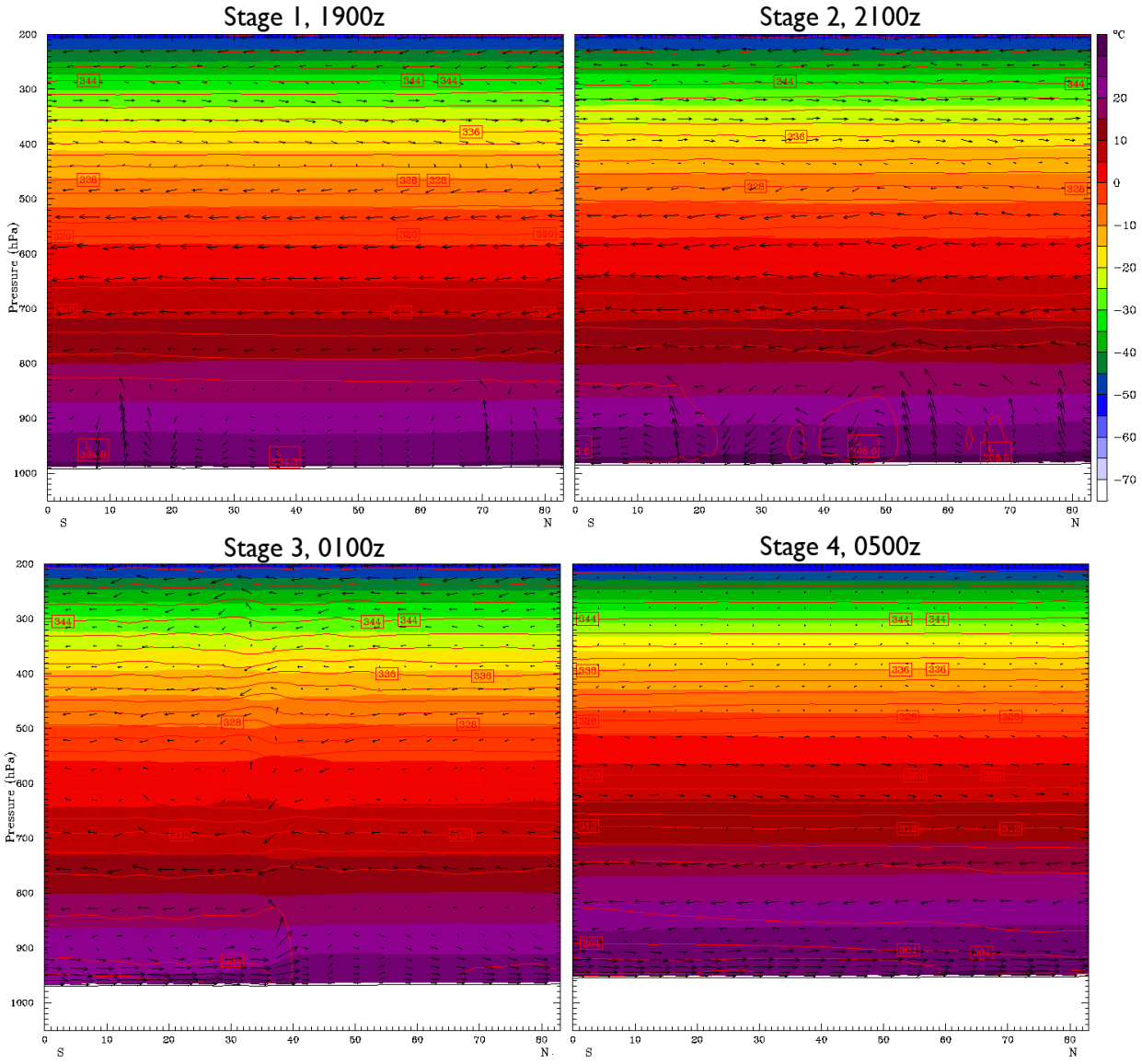

Fig. 4.10. Cross section views through the urban area from the SimpleUrban simulation showing the vertical distribution of temperature (colors, ºC) potential temperature (red contours, K) and the v and z components of wind velocity (vectors). The four stages of urban-coastal circulation are labeled.

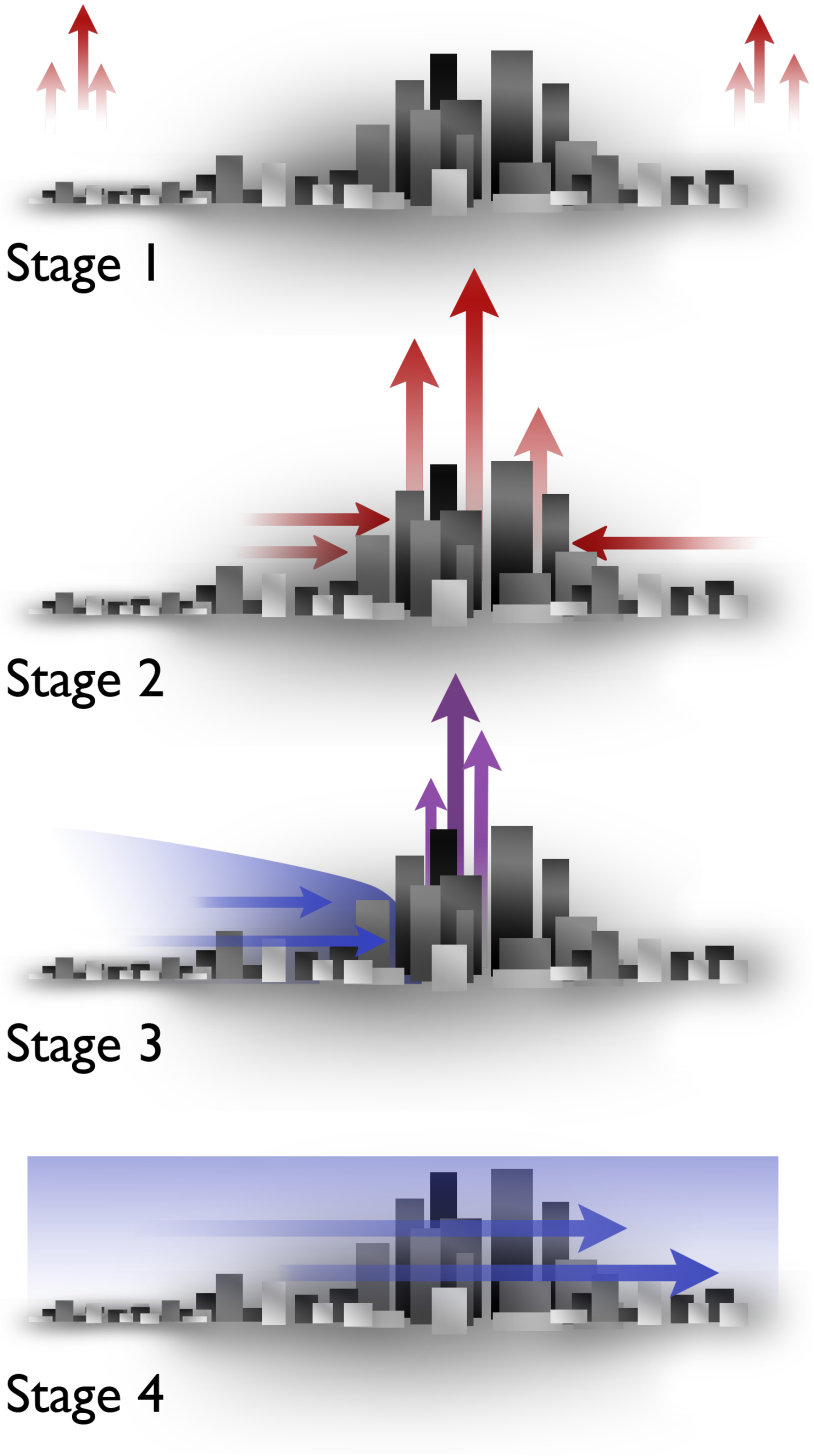

Fig. 4.11. Conceptual illustration of the evolution of urban-coastal circulations. Red represents urban-induced vertical motion, blue represents coastal forcing, and purple represents combined urban-coastal mechanisms.

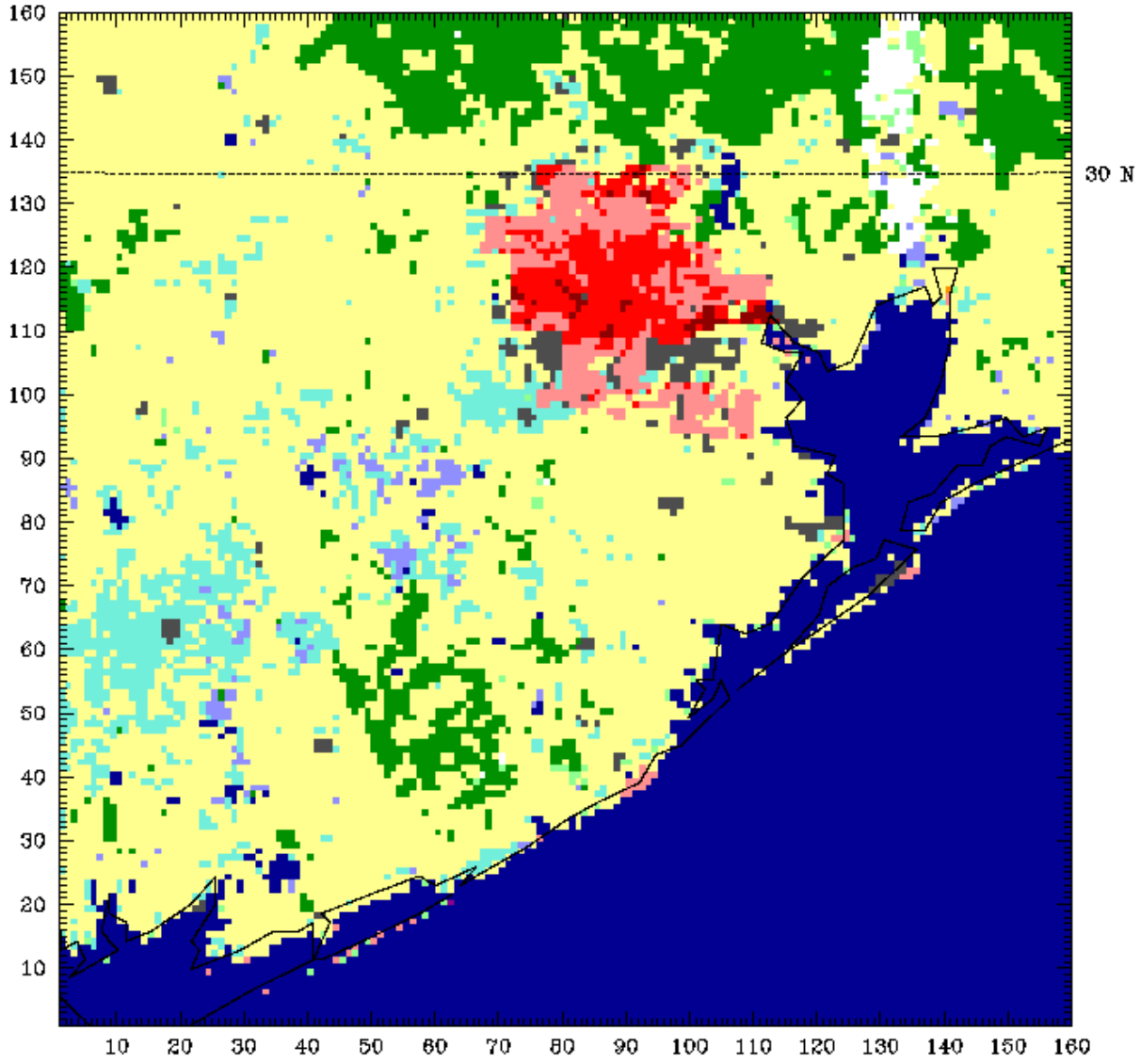

Fig. 4.12. Land cover data used to initialize WRF in the UCPUrban simulation. Urban areas for which enhanced UCPs were available are shown in shades of red, all other urban areas are shown in gray. Other land classes as in Fig. 3.1.

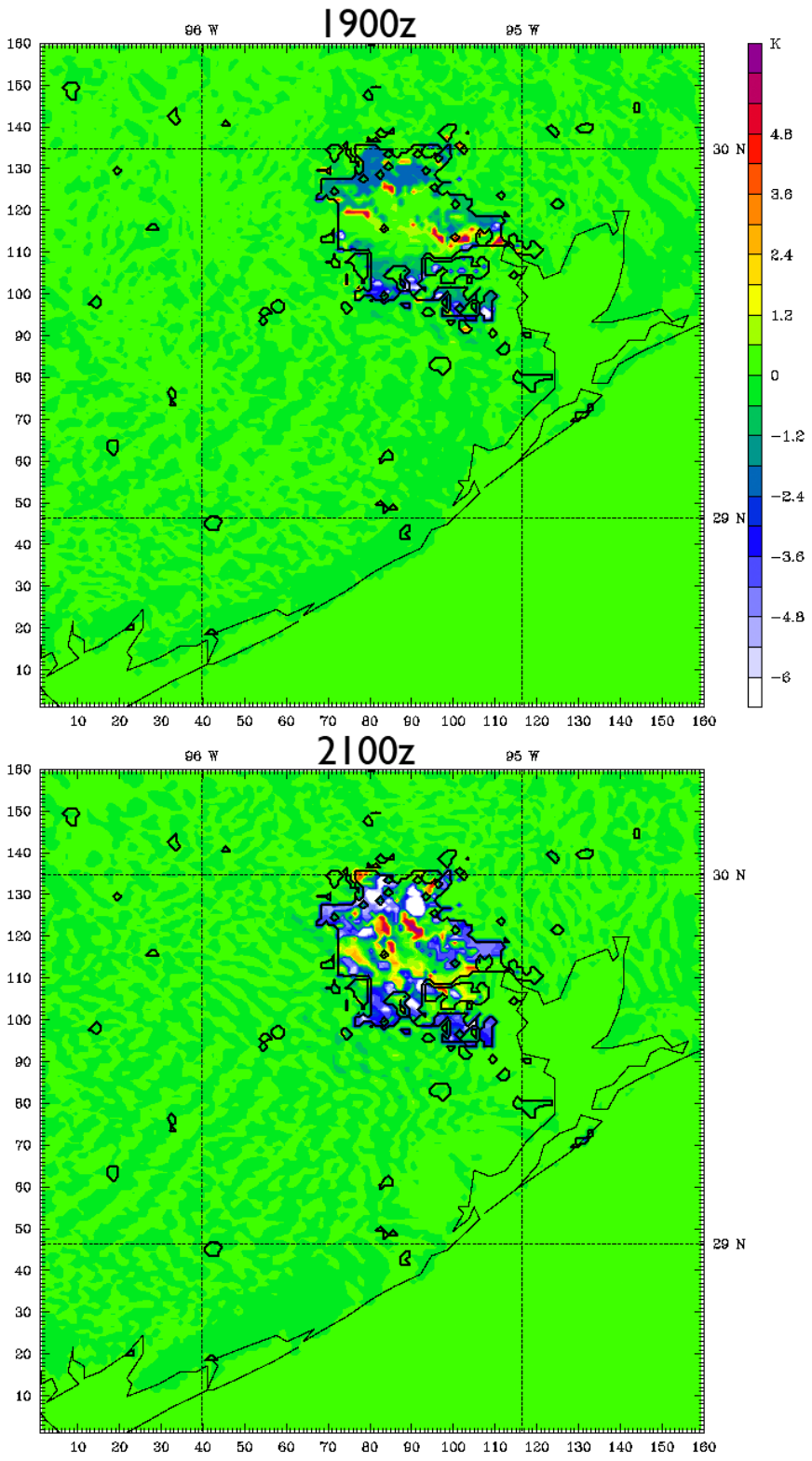

Fig. 4.13. Difference field resulting from the subtraction of the SimpleUrban skin temperature from the UCPUrban skin temperature (K) showing the complex differences which arise in skin temperature from the inclusion of enhanced urban canopy parameters.

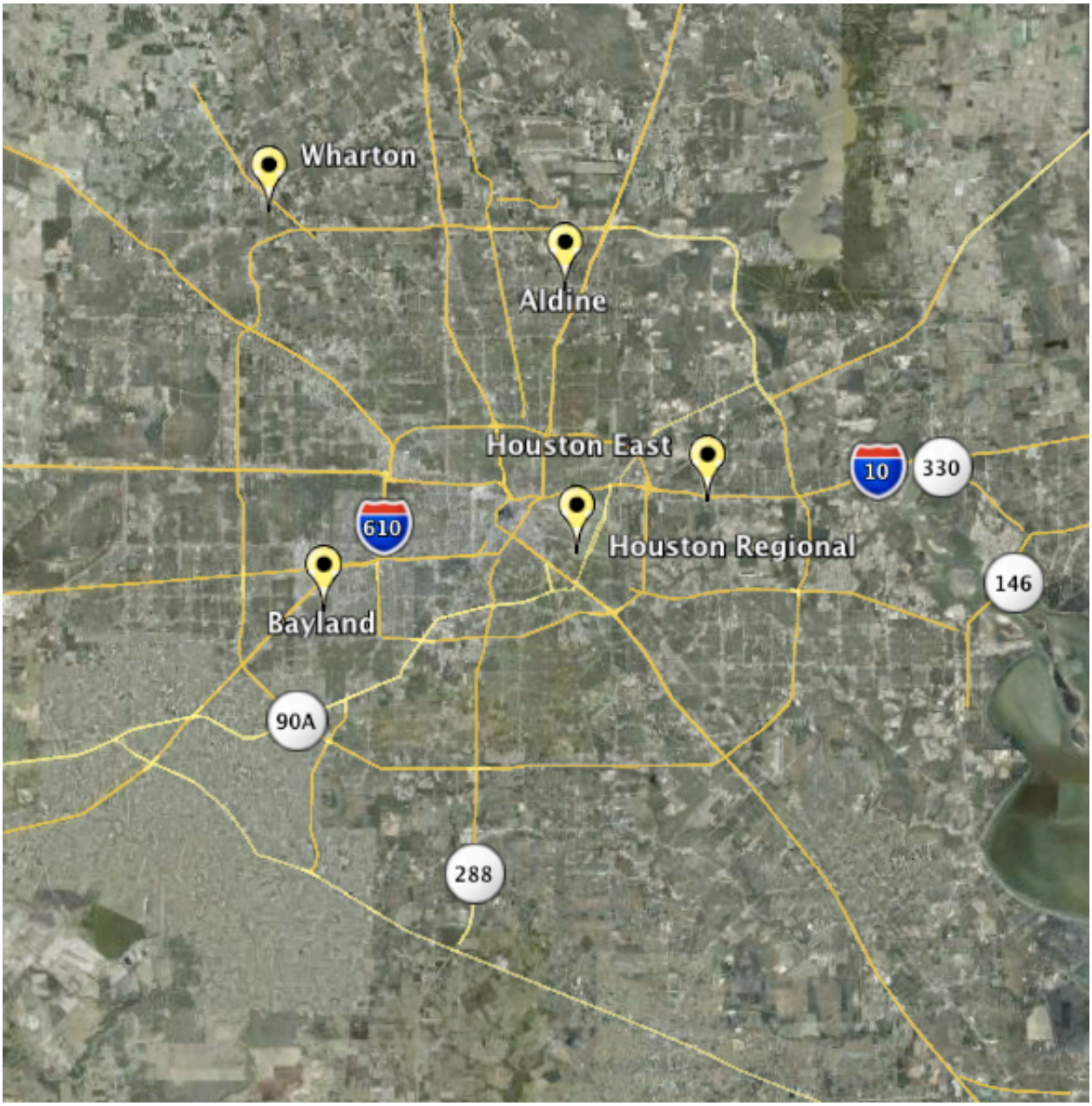

Fig. 4.14. Locations of the 5 TexAQS monitoring sites used to calculate the impact score of the urban canopy parameters.

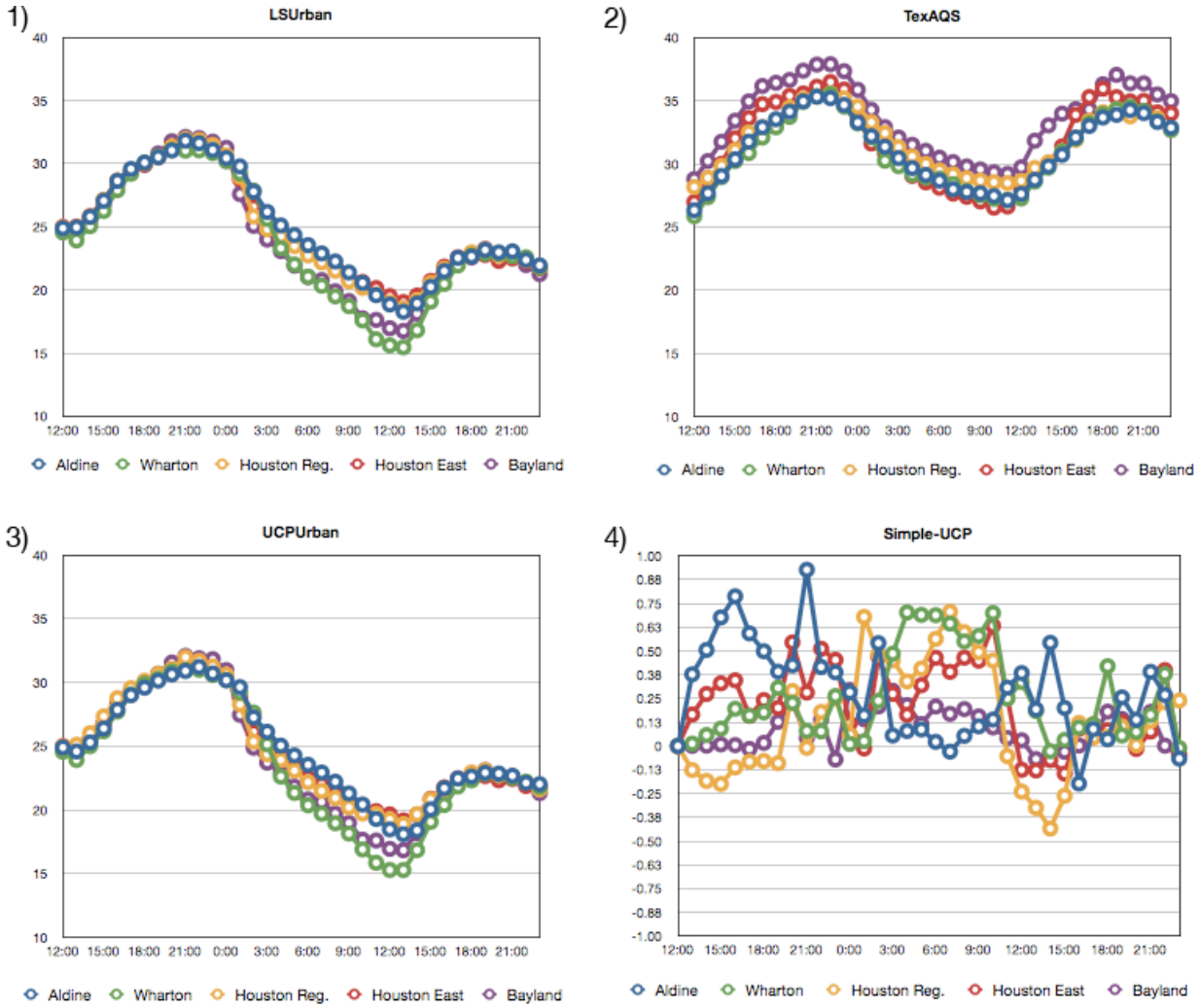

Fig. 4.15. Time series showing the 2m air temperature (ºC) from 1) the SimpleUrban simulation, 2) the UCP Urban Simulation, 3) the TexAQS field campaign measurements, and 4) the results of subtracting the SimpleUrban 2m air temperature from the UCP urban air temperature to illustrate the range of impacts from the inclusion of enhanced urban canopy parameters.

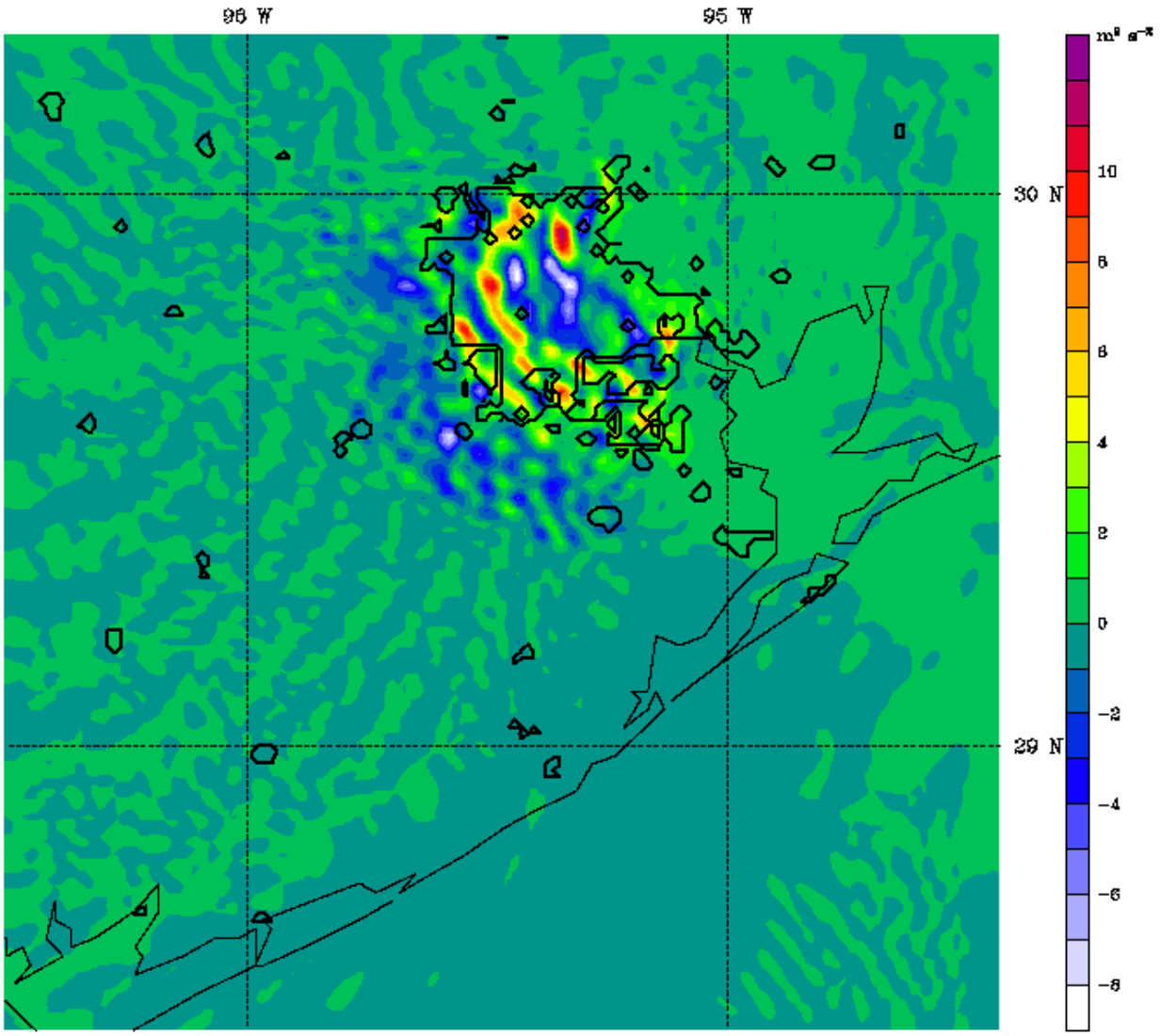

Fig. 4.16. Difference field resulting from the subtraction of the SimpleUrban BRN shear field from the UCPUrban BRN shear field (m^{-2} s^{-2}) at 2100 UTC (1600 CDT), illustrating the complex differences in the convective field caused by the inclusion of enhanced urban canopy parameters.

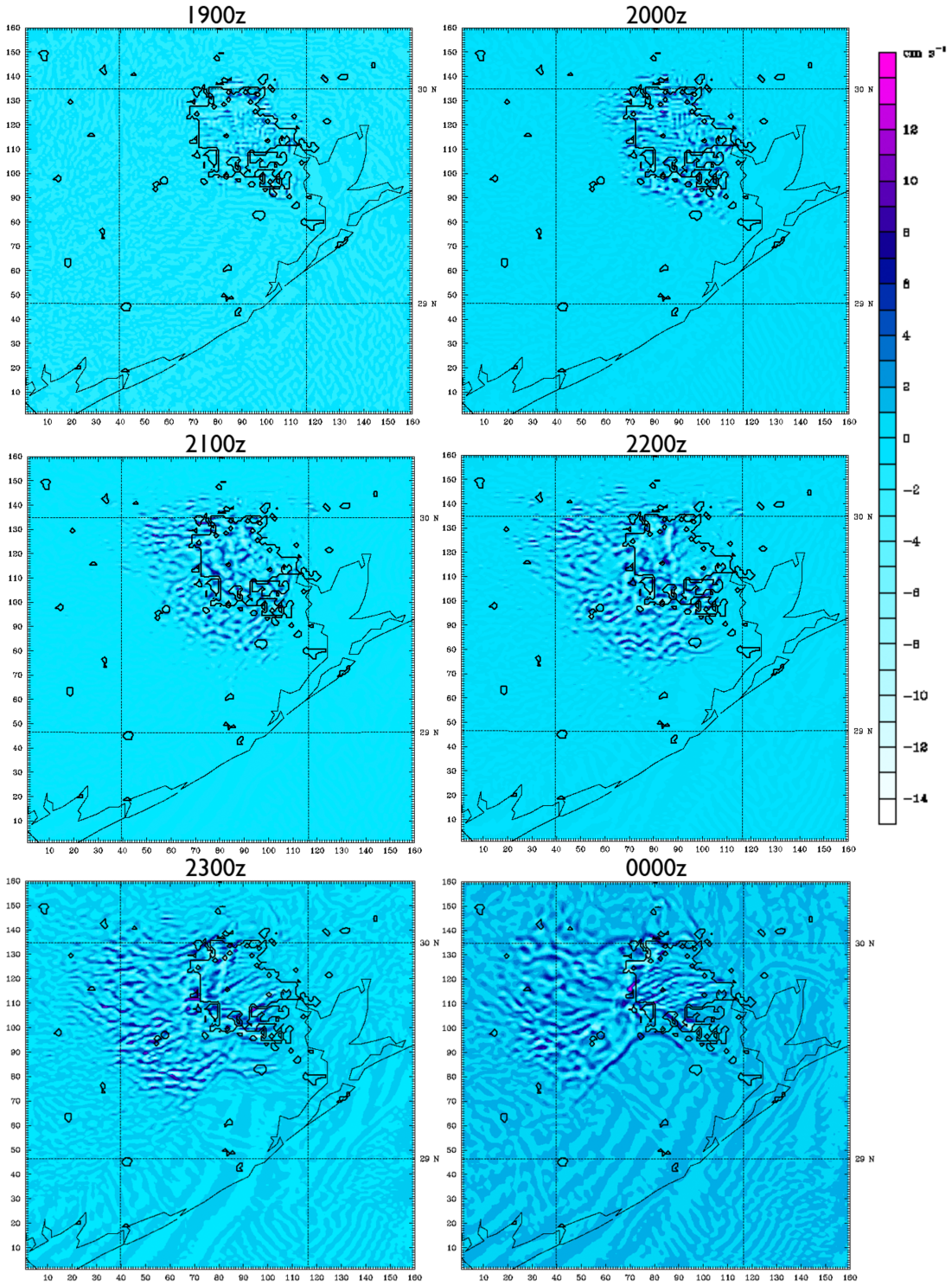

Fig. 4.17. Difference field resulting from the subtraction of the SimpleUrban near surface vertical velocity from the UCPUrban near surface vertical velocity (cm s^{-1}) from 1900 UTC – 0000 UTC (1400 – 1900 CDT). Of note is the westward propagation of vertical velocity anomalies affecting areas outside the urban environment.

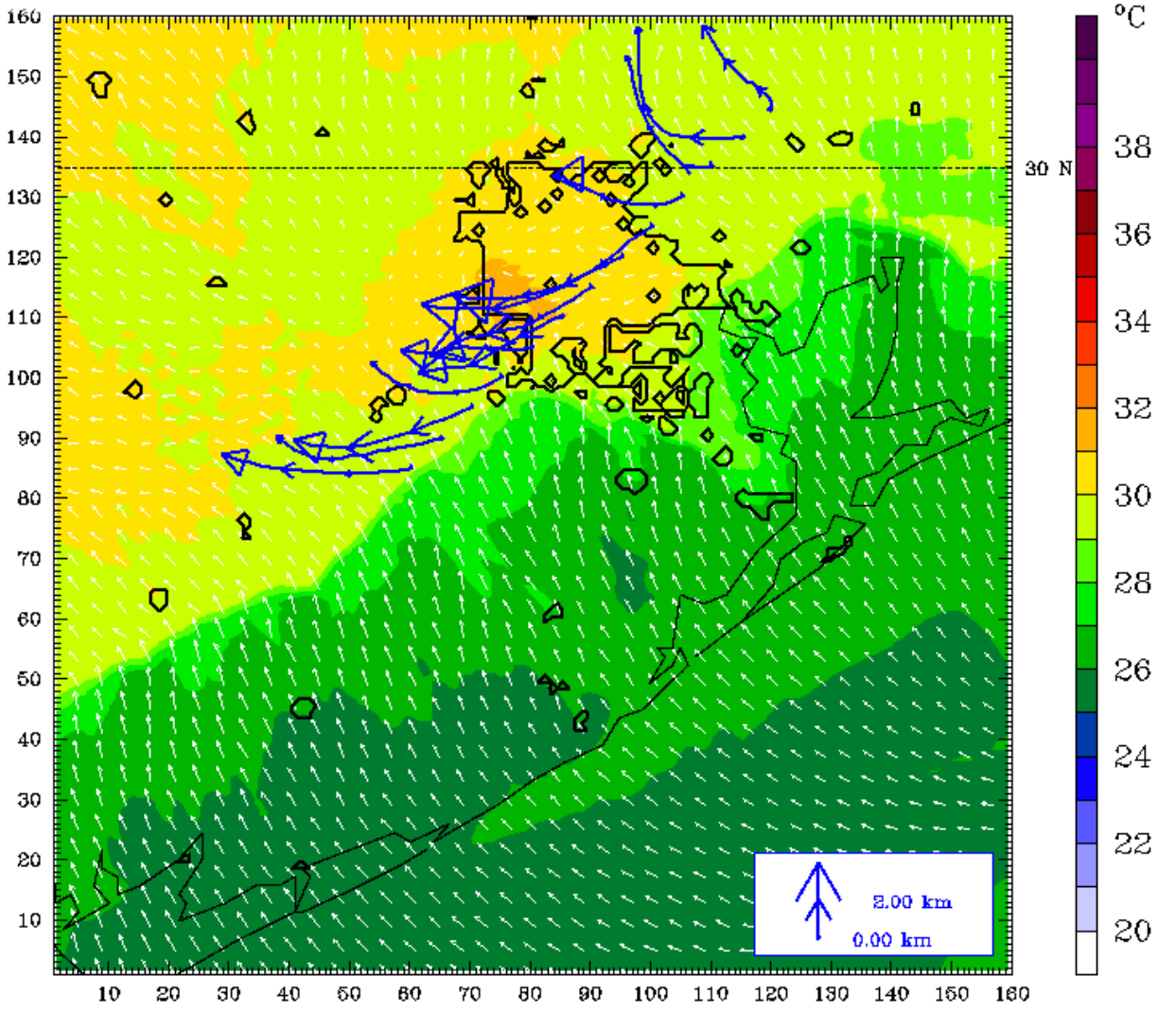

Fig. 4.18. Plot showing the trajectories of parcels released along a southwest to northeast transect through the urban area at 2100 UTC (1600 CDT), the time of convective pump initiation. The endpoints of each trajectory show the position of the parcel 0000 UTC (1900 CDT). Arrowhead size indicates altitude. Base map is 2m air temp (ºC) and wind vectors at 0000 UTC.

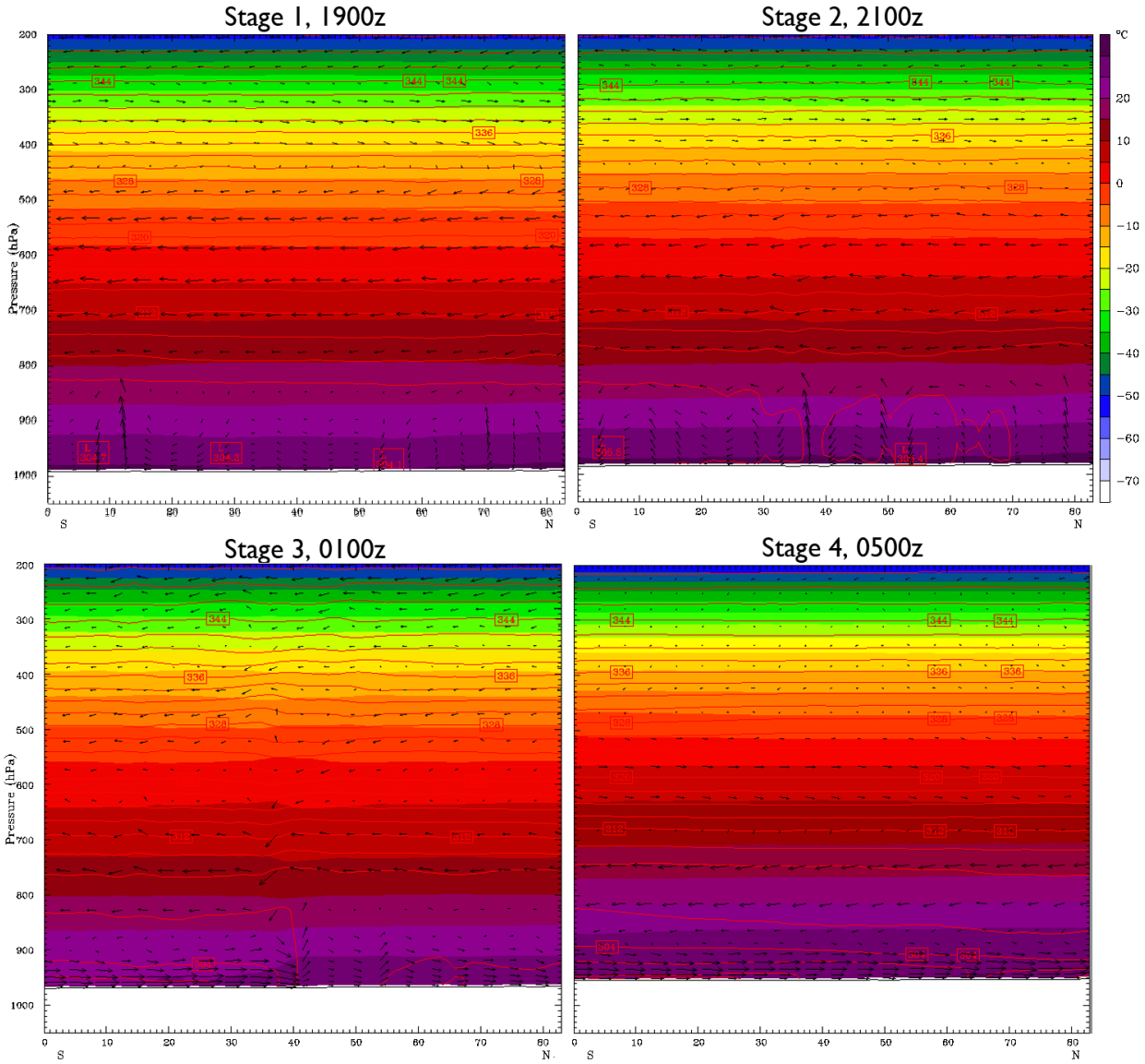

Fig. 4.19. Cross section views through the urban area from the UCPUrban simulation showing the vertical distribution of temperature (colors, ºC) potential temperature (red contours, K) and the v and z components of wind velocity (vectors). The four stages of urban-coastal circulation are labeled.

CHAPTER 5

CONCLUSIONS

This research has broad implications in the fields of urban weather, dispersion-transport, and climate, particularly regarding study of the expanding urban population centers near coastlines. As coastal cities become more densely populated, and heavy industry and residential areas are forced into closer contact, the effects of combined urban-coastal circulations on air quality and pollutant and contaminant transport become increasingly crucial to understand. This study has been able to characterize several important mechanisms that constitute the urban-coastal circulation. The sea breeze, urban heat island, and convective pump all contribute to this complex and interconnected system. The results presented show that it is possible to successfully model these circulations using modern numerical weather prediction systems and to enhance these simulations by incorporating high fidelity representation of the urban canopy. The following is a summary of the findings of this study.

5.1 The Convective Pump

Through a series of model simulations, this study has been able to characterize the structure and evolution of the convective pump generated by the city of Houston, TX. The convective pump is not dissimilar from the convective updrafts of thunderstorms. This study has therefore chosen to incorporate a parameter normally used to diagnose thunderstorm environments, the

BRN shear term, to identify and chart the evolution of the urban induced convective pump. The convective pump begins as a series of weak updrafts, with associated low level convergence and vertical velocity anomalies in the mid afternoon. It is believed that the primary forcing mechanism for the convective pump is the low level temperature anomaly caused by the increased skin temperature of urban surfaces, which provides the energy to destabilize the lower atmosphere. As the convective pump begins to mature, the diffuse low-level convective anomalies begin to organize into a coherent convective pump structure covering the entire urban area. At this stage the low level convergence and vertical velocity anomalies subside, while the BRN shear anomaly, which is able to capture a deeper layer of the atmosphere, remains strong. This suggests that the convective pump, once mature, begins to decouple from the surface. Thus, it appears that the most crucial aspect of the convective pump's evolution with regard to pollutant transport is its incipient phase, when it is in close contact with the surface and able to ingest material from urban pollutant sources or a chemical-biological-radiological release.

5.2 The Sea Breeze

The sea breeze is a long studied aspect of the coastal environment, but its interactions with urban centers have not been well understood. The implications of the sea breeze as a transport mechanism for pollutants are clear. Therefore in order to create a complete picture of transport in urban-coastal environments, understanding of the urban-influenced sea breeze is crucial. The results of these simulations show that while coastal morphology can itself lead to complex sea breeze front structures, including preferred areas of vertical motion, the urban environment also has a large impact on the evolution of the sea breeze mesoscale boundary. The sea breeze front

begins to strengthen and accelerate, particularly on the western edge of Houston, as it comes into contact with the urban area. This acceleration decreases the dwell time of the sea breeze front over the urban area, but also increases the strength of the vertical velocity anomaly. This "bulldozer effect" of the sea breeze front, combined with the vertical motions generated by the convective pump, could serve to concentrate atmospheric contaminants on the landward side of the boundary, as well as provide a strong south to north transport mechanism. Once the sea breeze front has passed, the stable marine airmass that follows in its wake can remain over the city through the morning of the next day. Pollutants released into this stable airmass would be trapped near the surface below the sea breeze induced low-level inversion, presenting a further concern for air quality or homeland security.

5.3 High Fidelity Representation of the Urban Canopy

This study shows the importance of high fidelity representation of the urban canopy to simulations of the urban-coastal environment. The inclusion of building heights and associated parameters into the model's land surface representation led to significant differences in patterns of skin surface temperature, which has implications for all aspects of urban weather. Comparison with observed 2m temperature shows that the inclusion of these enhanced UCPs improves the representation of low level air temperature within the model, especially where urban density is overestimated or underestimated by the standard urban land cover representation. Further, this change in skin temperature patterns leads to a higher degree of complexity in the evolution of the convective pump, especially during its incipient phase, which is the most important stage of its development with regard to pollutant transport. Areas where urban density is overestimated by

the standard representation, which tend to be residential, become preferred locations for pollutant transport in the enhanced urban scenario. The effects of enhanced urban canopy parameters are also not limited to the city itself. This analysis shows that perturbations generated by the enhanced urban environment begin to radiate outward from the city, preferentially to the west. This is particularly important for the evolution sea breeze front, which is most strongly affected by urban forcing on the western flank of the city.

5.4 Future Directions

This study has shown the continued importance of investigation into urban-coastal atmospheric processes. The high-resolution nature of these simulations has been shown to be crucial to resolving the complex patterns that emerge from the combination of urban and coastal forcing mechanisms. Further, the incorporation of advanced remote sensing techniques in generating urban canopy parameter data sets has proven to be useful. Future work in developing these data sets for use with other urban areas, as well as expanding the number of urban canopy parameters available within the data sets, will be necessary to explore this avenue of research to its full potential. Further field campaigns, such as TexAQS, will be an excellent resource for collecting model verification data with the goal of improving model performance. Future work investigating pollutant transport under different flow regimes could also make an important contribution for societal impacts and urban planning. Another possible use of this basic framework is the investigation of urban induced precipitation and lightning anomalies. Previous work has shown that urban areas are capable of affecting precipitation patterns over a large area, and better understanding of the urban induced convergence and vertical velocity structures

resolved by this study could lead to greater understanding of the forcing mechanisms which lead to these anomalies.

Coastal urban environments generate complex atmospheric forcing mechanisms. The circulations generated by these mechanisms alter dispersion and transport patterns of chemical, biological, and radiological agents and are of interest not only because of their implications for air quality and for accurate weather forecasting but because of potential homeland and national security concerns as well. It is hoped that this study will stand as a useful contribution toward greater understanding of the atmospheric circulations which result from urban-coastal interactions, and that this framework will lead to further improvements in our understanding of urban weather.

REFERENCES

Banta, R.M., C.J. Senff, J. Nielsen-Gammon, L.S. Darby, T.B. Ryerson, R.J. Alvarez, S.P. Sandberg, E.J. Williams, and M. Trainer, 2005: A bad air day in Houston. *Bull. Am. Met. Soc.*, **86,** 657-669.

Bornstein, R. D., and T. Oke, 1980: Influence of pollution on urban climatology. *Adv. Environ. Sci. Engineering*., **3,** 171-202.

Bornstein, R. D., 1987: Mean diurnal circulation and thermodynamic evolution of urban boundary layers. In *Modeling the Urban Boundary Layer*, American Meteor. Soc., Boston, 53–93.

Bornstein, R. D., and Q. Lin, 2000: Urban heat islands and summertime convective thunderstorms in Atlanta: three case studies. *Atmos. Environ.*, **34,** 507-516.

Burian, S.J.: Personal Communication. July 2, 2008.

Chen, F., Y. Liu, H. Kusaka, M. Tewari, J-W Bao, 2004: Utilizing the coupled WRF/LSM/urban modeling system with detailed urban classification to simulate the urban heat island phenomena over the greater Houston area. *Preprints Fifth Urban Environment Conference*, 23-27 August, Vancouver, Canada, Amer. Meteor. Soc.

Cowling, E.B., and Parrish, D., 2006: Preliminary findings from the second Texas Air Quality Study (TexAQS II). Report to the Texas Commission on Air Quality. 89 pp.

Crosett, K.M., Culliton, T.J., Wiley, P.C., Goodspeed, T.R. 2004: Population trends along the coastal United States: 1980-2008. US Department of Commerce Coastal Trends Reports Series. 54 pp.

Ek, M. B., K. E. Mitchell, Y. Lin, E. Rogers, P. Grummann,V. Koren, G. Gayno, and J. D. Tarpley, 2003: Implementation of NOAH land surface model advances in the National Centers for Environmental Prediction operational Mesoscale Eta Model. *J. Geophys. Res.*, **108,** 8851.

Glickman, T. S. (Ed.), 2000: *Glossary of Meteorology*. American Meteorological Society. 855 pp.

Grell, G.A., J. Dudhia, and D.R. Stauffer, 1994: A description of the fifth-gneneration Penn State/NCAR Mesoscale Model (MM5). NCAR Tech. Note NCAR/TN-398+STR. 122 pp.

Haurwitz, B. 1947: Comments on the sea-breeze circulation. *J. Meteor.,* **4**, 1-8.

Hjemfelt, M.R., 1982: Numerical simulation of the effects of St. Louis on mesoscale boundary layer airflow and vertical motion: Simulations of urban vs. non-urban effects., *J. Appl. Meteor*., **21**, 1239-1257.

Holton, J. R. *An Introduction to Dynamic Meteorology,* 4th ed. Academic Press, 511pp.

Holt, T., and Pullen, J, 2006: Urban canopy modeling of the New York City metropolitan area: A comparison and validation of single- and multilayer parameterizations. *Mon.Wea. Rev*., **135**, 1906-1930.

Howard, L., 1833: *Climate of London Deduced from Meteorological Observations*. 3rd ed., *Vol.1, Harvey and Darton, London,.* 348 pp.

Kitada, T., K. Okamura, and S. Tanaka, 1998: Effects of topography and urbanization on local winds and thermal environment in the Nohbi Plain, Coastal Region of Central Japan: A numerical analysis by mesoscale meteorological model with a *k*− turbulence model, *J. Appl. Meteor.*, **37**, 1026-1046

Kusaka, H. F. Kimura, H. Hirakuchi, and M. Mizutori, 2000: The effects of land-use alteration on the sea breeze and daytime heat island in the Tokyo metropolitan area*. J. Meteor. Soc. Japan*, **78**, 405-420.

Kusaka, H. and F. Kimura, 2004: Thermal effects of urban canyon structure on the nocturnal heat island: Numerical experiment using a mesoscale model coupled with an urban canopy model. *J. of Appl. Meteor.*, **43**, 1899-1910.

Lo, J.C.F., A.K.H. Lau, F. Chen, J.C.H. Fung, and K.K.M. Leung, 2007: Urban modification in a mesoscale model and the effects on the local circulation in the Pearl River Delta region. *J. Appl. Meteor. Climatol*., **46**, 457–476.

Manley, G., 1958: On the frequency of snowfall in metropolitan England. *Q. J. Roy. Meteor. Soc.*, **84,** 70–72.

McPherson, R. D., 1970: A numerical study of the effect of a coastal irregularity on the sea breeze. *J. Appl. Meteor.*, **9**, 767-777.

Nielsen-Gammon, J. W., 2000: The Houston heat pump: modulation of a land-sea breeze by an urban heat island. Presentation to the 2000 PSU/NCAR Mesoscale Modeling System Users' Workshop. http://box.mmm.ucar.edu/mm5/workshop/workshop-program-2000.html

Nielsen-Gammon, J. W.: Personal Communication. January 11, 2009.

Ohashi, Y., and H. Kida, 2002: Local circulations developed in the vicinity of both coastal and inland urban areas: Numerical study with a mesoscale atmospheric model. *J. Appl. Meteor*., **41**, 30-45**.**

Oke, T.R., 1981: Canyon geometry and nocturnal urban heat island: Comparison of scale model and field observations. *J. Climatol.,* **1**, 237-254.

Oke, T.R., 1987: *Boundary Layer Climates 2nd Ed.* Methuen Co., New York. 435 pp.

Rozoff, C., William R. Cotton and Jimmy O. Adegoke. 2003: Simulation of St. Louis, Missouri, land use impacts on thunderstorms. *J. of Appl. Meteor.* **42**, 716–738

Shem, W., and J.M. Shepherd, 2009: On the impact of urbanization on summertime thunderstorms in Atlanta: Two numerical model case studies. *Atmospheric Research*, Atmospheric Research, **92**, 172-189.

Shepherd, J.M., Brad S. Ferrier, and Peter S. Ray, 2001: Rainfall morphology in Florida convergence zones: A numerical study, *Mon. Wea. Rev.*, **129**, 177-197.

Shepherd, J.M. 2005: A review of current investigations of urban-induced rainfall and recommendations for the future. *Earth Interactions*, **9**, 1–27.

Shepherd, J.M., W.M. Carter, M. Manyin, D. Messen, and S. Burian, 2009: The impact of urbanization on current and future coastal convection: A case study for Houston, *Environment And Planning B,* submitted.

Simpson, J. E., 1994: *Sea Breeze and Local Wind*. Cambridge University Press, 234 pp.

Simpson, M. D., 2006: Role of urban land use on mesoscale circulations and precipitation. PhD dissertation, North Carolina State University, 294 pp.

Skamarock, W. C., Klemp, J. B., Dudhia, J., Gill, D. O., Barker, D. M., Wang, W., Powers, J. G. 2007: A description of the advanced research WRF version 2. NCAR Tech. Note NCAR/ TN–468+STR. 88 pp.

Souch, C., and S. Grimmond, 2006: Applied climatology: Urban climate. *Progress in Physical Geogr*., **30,** 270-279.

Tewari, M., F. Chen, H. Kusaka, and S. Mio, 2007: *Coupled WRF/Unified NOAH/Urban-Canopy Modeling System*. NCAR Research Applications Laboratory. Available at www.rap.ucar.edu/research/. 22pp.

United Nations Population Fund. *2007 Annual Report*. UNFPA Information and External Relations Division. Available at www.unfpa.org. 30 pp.

Weisman, M.L., and J.B. Klemp, 1982: The dependence of numerically simulated convective storms on vertical wind shear and buoyancy. *Mon. Wea. Rev.*, **110**, 504-520

Yoshikado, H., 1992: Numerical study of the daytime urban effect and its interaction with the sea breeze. *J. Appl. Meteor*., **31**, 1146-1164.

Yoshikado, H., 1994: Interaction of the sea breeze with urban heat islands of different sizes and locations. *J. Meteor. Soc. Japan*, **72**, 139-142.